4. Earthquake deformation

- Representation of seismic source
- Theory of coseismic deformation
- Coseismic deformation
- Interseismic deformation
- Postseismic deformation
- Earthquake cycle
- Slow earthquake
- Static stress change

4.1. Representation of seismic source

- Earthquake: spontaneous rupture in the earth caused by internal forces
- Such forces should have no-net-force and no-net-torque.
- Moment tensor describes amplitude of such force systems

4.1. Representation of seismic source

- Moment tensor
  - Describe strength of 9 coupled force systems
  - Each force system satisfies no-net-force condition
  - Symmetric: satisfy no-net-torque condition
  - Equivalent description of inelastic deformation at source region

$$M = \begin{pmatrix} M_{xx} & M_{xy} & M_{xz} \\ M_{xy} & M_{yy} & M_{yz} \\ M_{xz} & M_{yz} & M_{zz} \end{pmatrix}$$

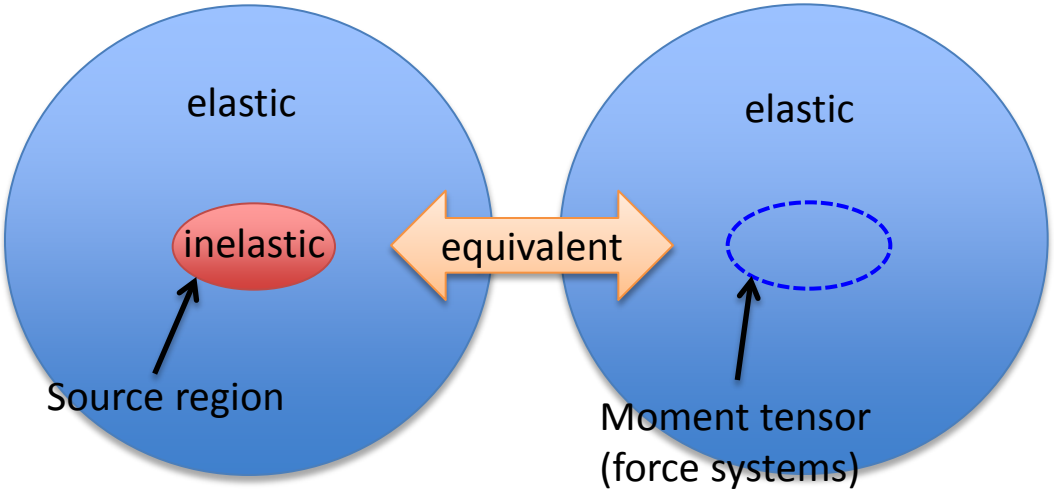

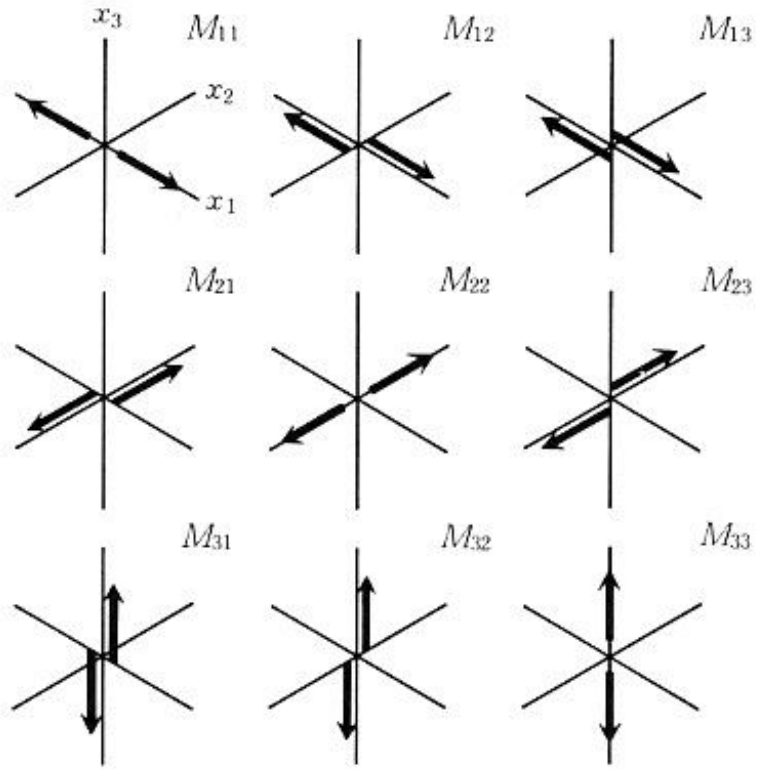

4.1. Representation of seismic source

- Moment tensor
  - Shear component only (no volumetric change) ➔ trace(***M***)=0
  - In such a case, moment tensor can be transformed into the following form by proper rotation of coordinate axes.

$$\begin{pmatrix} 0 & 0 & M_0 \\ 0 & 0 & 0 \\ M_0 & 0 & 0 \end{pmatrix}$$

  - M_0 in the above expression is called “seismic moment”, which is a good measure about the size of an earthquake

$$M_0 = \mu DS$$

$$\log M_0 = 1.5 M_w + 9.1$$

4.1. Representation of seismic source

- Double couple force system
  - seismological analysis

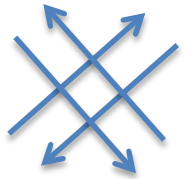

Equivalent

- Fault slip
  - observation of surface faulting

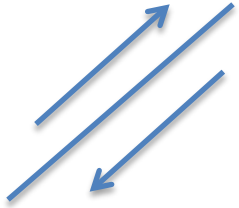

Burridge and Knopoff (1963)

Faulting is earthquake source

(Photo: Active Fault and Earthquake Research Center,
National Institute of Advanced Industrial Science and Technology)

4.2. Theory of coseismic deformation

- Theoretical formula to describe deformation due to buried fault in an elastic medium is derived based on the **dislocation theory**.
- 'Dislocation' or displacement discontinuity across the fault is equal to the fault slip.

$$\Delta u = u^{+} - u^{-}$$

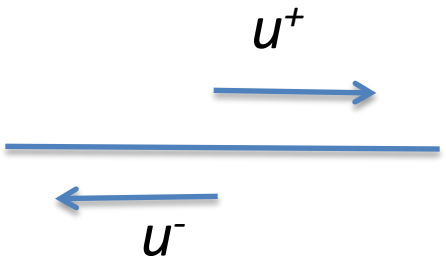

- Assumptions:
  - Homogeneous elastic half-space
  - Source
    - Point source
    - Rectangular fault (uniform slip)
  - Linear elasticity: Effects of multiple sources can be superimposed

4.2. Theory of coseismic deformation

- Example: Infinitely long strike slip fault
  - Uniform slip between z=-d_1 and z=-d_2
  - Only y-component displacement exists
  - Deformation at all depth

$$u_y = \frac{s}{2\pi}\left\{\tan^{-1}\left(\frac{x}{z+d_1}\right)-\tan^{-1}\left(\frac{x}{z-d_1}\right)-\tan^{-1}\left(\frac{x}{z+d_2}\right)+\tan^{-1}\left(\frac{x}{z-d_2}\right)\right\}_S$$

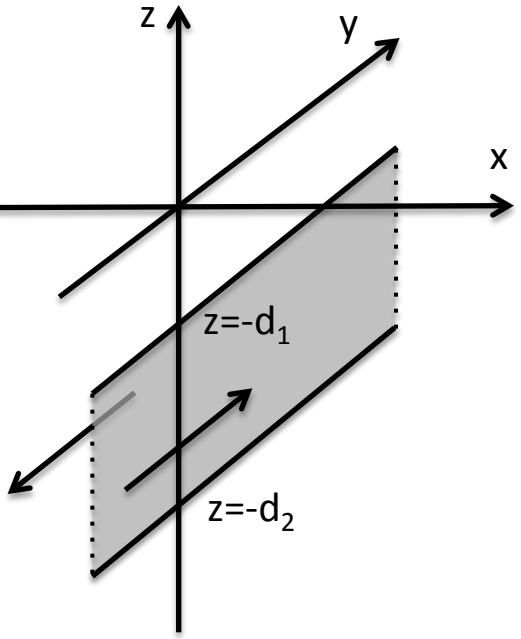

  - Surface displacement (z=0)

$$u_y = \frac{s}{\pi}\left\{\tan^{-1}\left(\frac{x}{d_1}\right)-\tan^{-1}\left(\frac{x}{d_2}\right)\right\}$$

$d_1 \rightarrow 0$ $\quad u_y = \frac{s}{\pi}\tan^{-1}\left(\frac{d_2}{x}\right)$

$d_2 \rightarrow \infty$ $\quad u_y = \frac{s}{\pi}\tan^{-1}\left(\frac{x}{d_1}\right)$

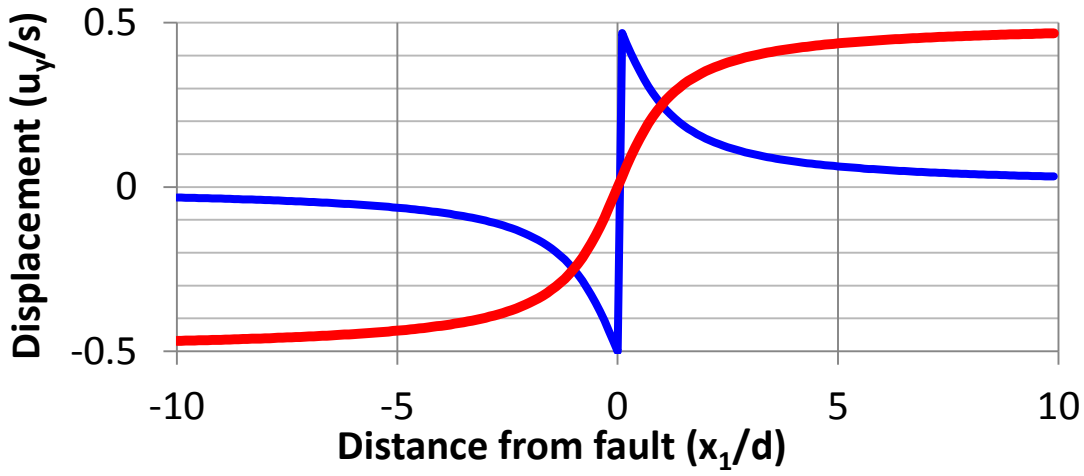

4.2. Theory of coseismic deformation

- General Formula to describe coseismic deformation of elastic half space
- Surface deformation
  - Point source
    - Stekettee (1958), Maruyama (1964), Okada (1985)
  - Finite source
    - Chinnery (1961), Manshinha and Smylie (1971), Okada (1985)
- Internal deformation
  - Point source
    - Stekettee (1958), Maruyama (1964), Iwasaki and Sato (1979)
  - Finite source
    - Chinnery (1961), Manshinha and Smylie (1971), Iwasaki and Sato (1979), Okada (1992)

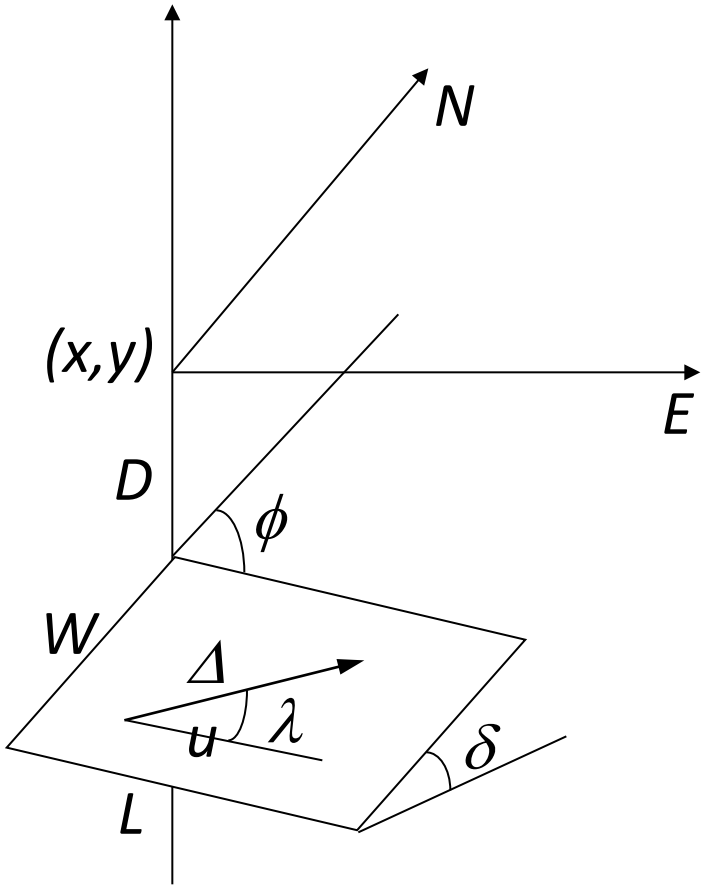

4.2. Theory of coseismic deformation

- Point source
  - Strike slip

$$\begin{cases} u_x^0 = -\dfrac{U_1}{2\pi}\left[\dfrac{3x^2q}{R^5} + I_1^0 \sin\delta\right]\Delta\Sigma \\ u_y^0 = -\dfrac{U_1}{2\pi}\left[\dfrac{3xyq}{R^5} + I_2^0 \sin\delta\right]\Delta\Sigma \\ u_z^0 = -\dfrac{U_1}{2\pi}\left[\dfrac{3xdq}{R^5} + I_4^0 \sin\delta\right]\Delta\Sigma \end{cases}$$

  - Dip slip

$$\begin{cases} u_x^0 = -\dfrac{U_2}{2\pi}\left[\dfrac{3xpq}{R^5} - I_3^0 \sin\delta\cos\delta\right]\Delta\Sigma \\ u_y^0 = -\dfrac{U_2}{2\pi}\left[\dfrac{3ypq}{R^5} - I_1^0 \sin\delta\cos\delta\right]\Delta\Sigma \\ u_z^0 = -\dfrac{U_2}{2\pi}\left[\dfrac{3dpq}{R^5} - I_5^0 \sin\delta\cos\delta\right]\Delta\Sigma \end{cases}$$

  - Tensile slip

$$\begin{cases} u_x^0 = \dfrac{U_3}{2\pi}\left[\dfrac{3x^2q}{R^5} - I_3^0 \sin^2\delta\right]\Delta\Sigma \\ u_y^0 = \dfrac{U_3}{2\pi}\left[\dfrac{3yq^2}{R^5} - I_1^0 \sin^2\delta\right]\Delta\Sigma \\ u_z^0 = \dfrac{U_3}{2\pi}\left[\dfrac{3dq^2}{R^5} - I_5^0 \sin^2\delta\right]\Delta\Sigma \end{cases}$$

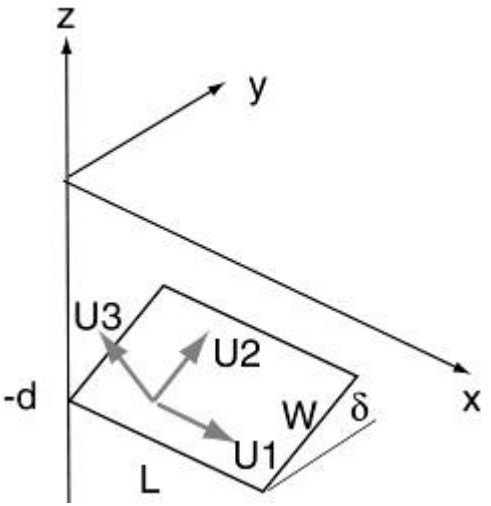

$$\begin{cases} I_1^0 = \dfrac{\mu}{\lambda+\mu} y\left[\dfrac{1}{R(R+d)^2} - x^2\dfrac{3R+d}{R^3(R+d)^3}\right] \\ I_2^0 = \dfrac{\mu}{\lambda+\mu} x\left[\dfrac{1}{R(R+d)^2} - y^2\dfrac{3R+d}{R^3(R+d)^3}\right] \\ I_3^0 = \dfrac{\mu}{\lambda+\mu}\dfrac{x}{R^3} - I_2^0 \\ I_4^0 = \dfrac{\mu}{\lambda+\mu}\left[-xy\dfrac{2R+d}{R^3(R+d)^2}\right] \\ I_5^0 = \dfrac{\mu}{\lambda+\mu}\left[\dfrac{1}{R(R+d)} - x^2\dfrac{2R+d}{R^3(R+d)^2}\right] \end{cases}$$

$\Delta\Sigma$: defined so that $\mu U \Delta\Sigma$ to be the double couple moment

4.2. Theory of coseismic deformation

- Rectangular fault
  - Strike slip

$$\begin{cases} u_x = -\dfrac{U_1}{2\pi}\left[\dfrac{\xi q}{R(R+\eta)} + \tan^{-1}\dfrac{\xi\eta}{qR} + I_1\sin\delta\right] \\ u_y = -\dfrac{U_1}{2\pi}\left[\dfrac{\tilde{y} q}{R(R+\eta)} + \dfrac{q\cos\delta}{R+\eta} + I_2\sin\delta\right] \\ u_z = -\dfrac{U_1}{2\pi}\left[\dfrac{\tilde{d} q}{R(R+\eta)} + \dfrac{q\sin\delta}{R+\eta} + I_4\sin\delta\right] \end{cases}$$

  - Dip slip

$$\begin{cases} u_x = -\dfrac{U_2}{2\pi}\left[\dfrac{q}{R} - I_3\sin\delta\cos\delta\right] \\ u_y = -\dfrac{U_2}{2\pi}\left[\dfrac{\tilde{y} q}{R(R+\xi)} + \cos\delta\tan^{-1}\dfrac{\xi\eta}{qR} - I_1\sin\delta\cos\delta\right] \\ u_z = -\dfrac{U_2}{2\pi}\left[\dfrac{\tilde{d} q}{R(R+\xi)} + \sin\delta\tan^{-1}\dfrac{\xi\eta}{qR} - I_5\sin\delta\cos\delta\right] \end{cases}$$

  - Tensile slip

$$\begin{cases} u_x = \dfrac{U_3}{2\pi}\left[\dfrac{q^2}{R(R+\eta)} - I_3\sin^2\delta\right] \\ u_y = \dfrac{U_3}{2\pi}\left[\dfrac{-\tilde{d} q}{R(R+\xi)} - \sin\delta\left\{\dfrac{\xi q}{R(R+\eta)} - \tan^{-1}\dfrac{\xi\eta}{qR}\right\} - I_1\sin^2\delta\right] \\ u_z = \dfrac{U_3}{2\pi}\left[\dfrac{\tilde{y} q}{R(R+\xi)} + \cos\delta\left\{\dfrac{\xi q}{R(R+\eta)} - \tan^{-1}\dfrac{\xi\eta}{qR}\right\} - I_5\sin^2\delta\right] \end{cases}$$

$$f(\xi,\eta)\Big|\equiv f(x,p) - f(x,p-W) - f(x-L,p) + f(x-L,p-W)$$

$$\begin{cases} I_1 = \dfrac{\mu}{\lambda+\mu}\left[\dfrac{-1}{\cos\delta}\dfrac{\xi}{R+\tilde{d}}\right] - I_5\tan\delta \\ I_2 = \dfrac{\mu}{\lambda+\mu}\left[-\ln(R+\eta)\right] - I_3 \\ I_3 = \dfrac{\mu}{\lambda+\mu}\left[\dfrac{1}{\cos\delta}\dfrac{\tilde{y}}{R+\tilde{d}} - \ln(R+\eta)\right] + I_4\tan\delta \\ I_4 = \dfrac{\mu}{\lambda+\mu}\dfrac{1}{\cos\delta}\left[\ln(R+\tilde{d}) - \sin\delta\ln(R+\eta)\right] \\ I_5 = \dfrac{\mu}{\lambda+\mu}\dfrac{2}{\cos\delta}\tan^{-1}\dfrac{\eta(X+q\cos\delta)+X(R+X)\sin\delta}{\xi(R+X)\cos\delta} \end{cases}$$

If $\cos\delta=0$

$$\begin{cases} I_1 = -\dfrac{\mu}{2(\lambda+\mu)}\dfrac{\xi q}{(R+\tilde{d})} \\ I_3 = \dfrac{\mu}{2(\lambda+\mu)}\left[\dfrac{\eta}{R+\tilde{d}} + \dfrac{\tilde{y} q}{(R+\tilde{d})} - \ln(R+\eta)\right] \\ I_4 = -\dfrac{\mu}{\lambda+\mu}\dfrac{q}{(R+\tilde{d})} \\ I_5 = -\dfrac{\mu}{\lambda+\mu}\dfrac{\xi\sin\delta}{(R+\tilde{d})} \end{cases}$$

$$\begin{cases} p = y\cos\delta + d\sin\delta \\ q = y\sin\delta - d\cos\delta \\ \tilde{y} = \eta\cos\delta + q\sin\delta \\ \tilde{d} = \eta\sin\delta - q\cos\delta \\ R^2 = \xi^2 + \eta^2 + q^2 = \xi^2 + \tilde{y}^2 + \tilde{d}^2 \\ X^2 = \xi^2 + q^2 \end{cases}$$

4.2 Theory of coseismic deformation

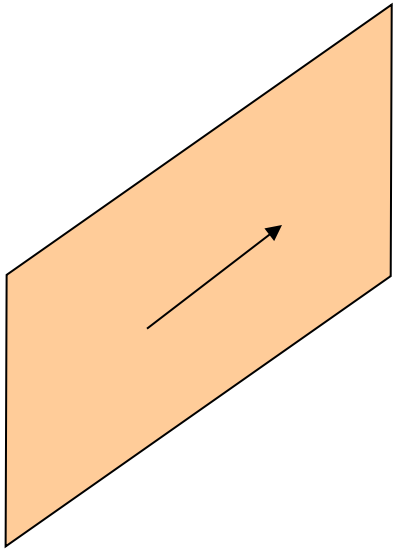

Single Fault

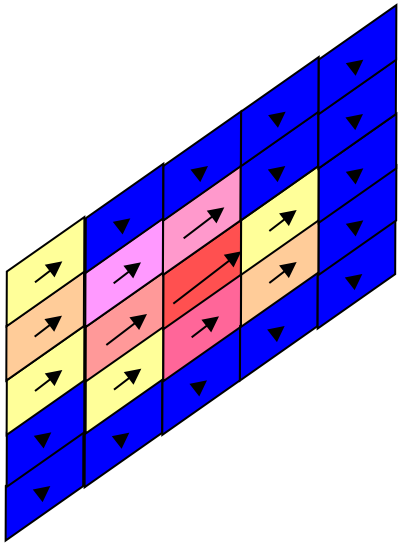

Multi-rectangular Fault model

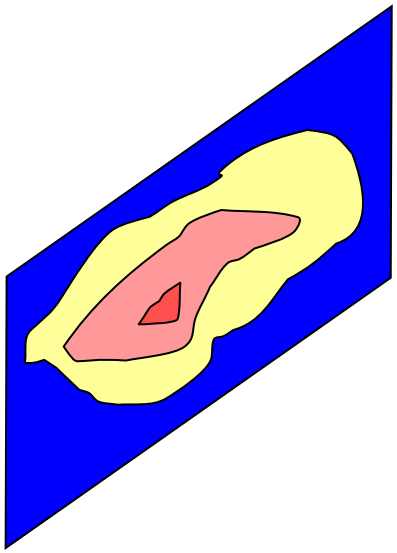

Smooth slip distribution

- Actual fault slip distribution is never homogeneous
- Dense observation data allows higher spatial resolution of fault slip distribution
- Inhomogeneous slip distribution can be described as linear superposition of basis functions
- Contribution from each subfault or basis function can be simply imposed to obtain total displacement

4.3. Coseismic deformation

1927 Tango (M7.3)

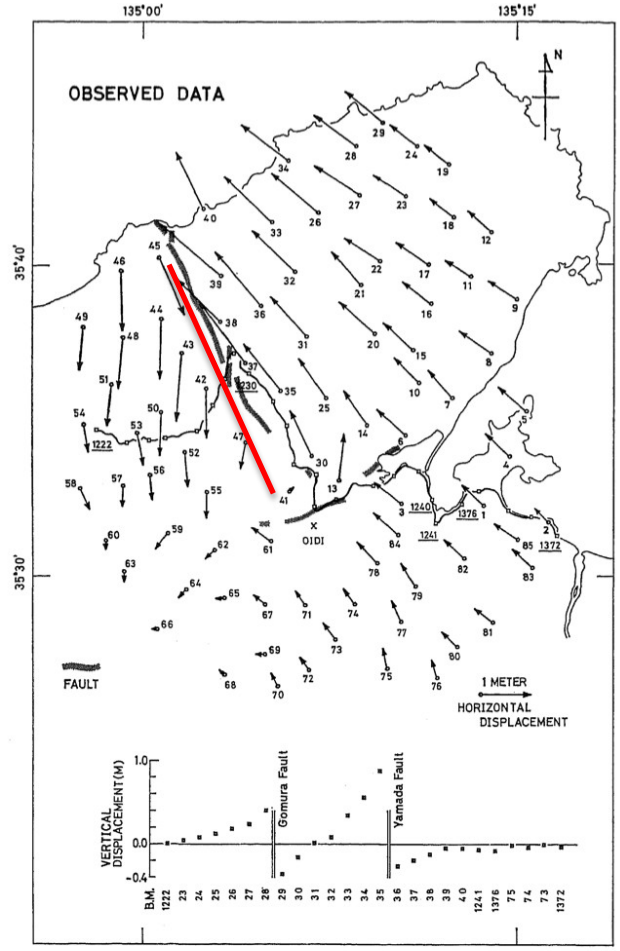

Fig. 1. Static deformations due to the 1927 Tango earthquake. Only 85 triangulation and 25 levelling data are shown, which are used in the present analysis. Each station number corresponds to that in Table 2.

Vertical strike slip fault

(Matsu'ura, Inversion of Geodetic. PART II. "Optimal Model of Conjugate Fault System for the 1927 Tango Earthquake", Journal of Physics of the Earth, Vol. 25, No.3, 1977)

2003 Tokachi-oki (M8.3)

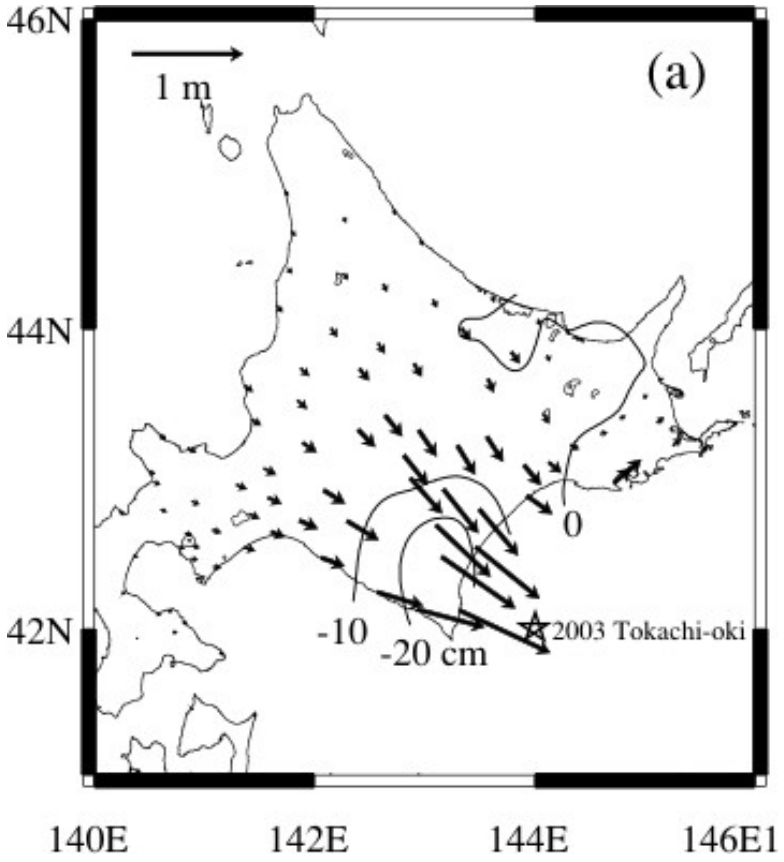

Low-angle thrust fault

(Ozawa et. al, "Coseismic and Postseismic Crustal Deformation after the Mw 8 Tokachi-oki Earthquake in Japan", Earth Planets Space, 56, 675–680, 2004)

4.3. Coseismic deformation

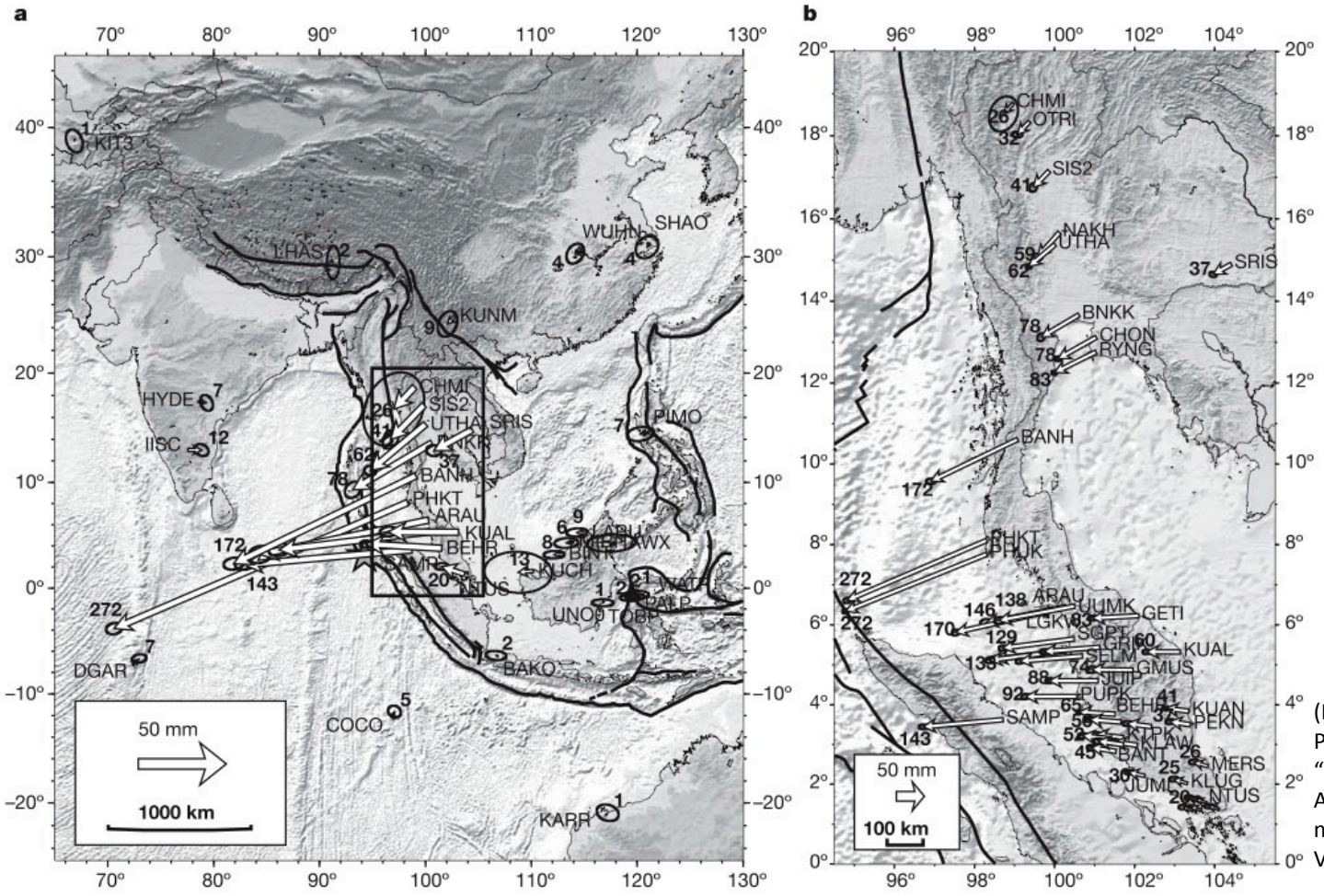

(Permission from Macmillan Publishers Ltd: Nature, "Insight into the 2004 Sumatra-Andaman earthquake from GPS measurements in southeast Asia", Vigny et al., 2005.)

Figure 1 | Co-seismic displacement field derived from GPS observations at more than 60 sites. Panel **a** shows a large scale overview from a low-density subset. Panel **b** provides more detail, zooming in on a smaller area (rectangular box in **a**). Note the high-density sub-network on the Malaysian peninsular. Bold numbers next to arrow heads give the displacement in mm. Ellipses depict the 90% confidence level. Thin black lines depict major faults[8]. The USGS earthquake epicentre location is portrayed by the star symbol, near bottom left of box. ETOPO-5 and GTOPO-30 Digital Elevation Models were used to generate the background topography and bathymetry.

Coseismic deformation was detected over large distances (>2000km). Sphericity of the earth should be considered in the interpretation.

4.3. Coseismic deformation

1999 Izumit earthquake (Turkey)
Typical strike slip faulting

4.3. Coseismic deformation

- 1995 Kobe earthquake
  - Consistency between geodetic and seismological data analysis

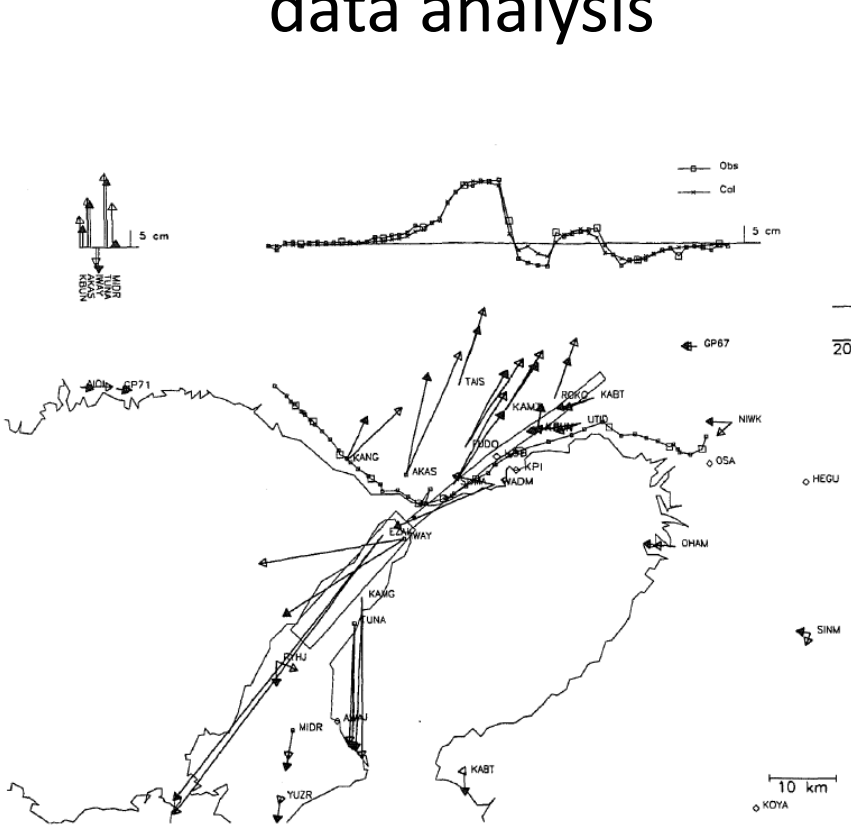

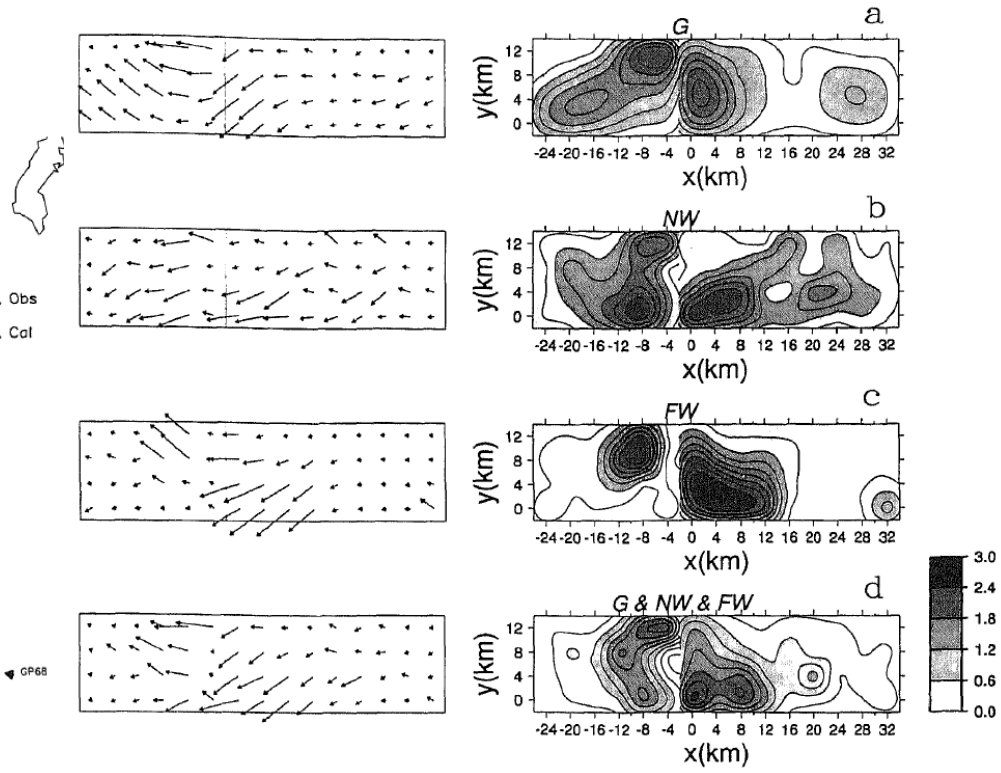

(Yoshida et. al, "Joint Inversion of the Near- and Far-Field Waveforms and Geodetic Data for the Rupture Process of the 1995 Kobe Earthquake", Journal of Physics of the Earth, 44, 437--454, 1996.)

4.3 Coseismic deformation

- Sometimes an earthquake occurring close to the trench causes a large tsunami compared with its magnitude.
- Such an earthquake is called “Tsunami earthquake”
- The tip of the continental part is “accretionary prism” where elastic constant is generally small
- Because of its small rigidity, this part may cause larger slip for the same seismic moment.
- This may be a candidate mechanism of tsunami earthquake.

$$M_0 = \mu DS$$ Small μ ➔ large D for same M_0

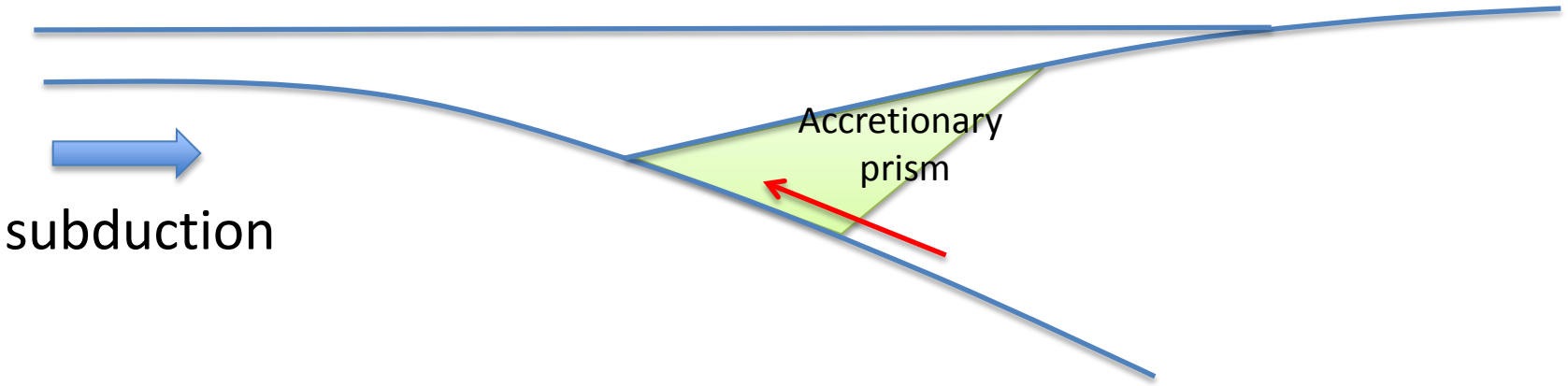

4.4. Interseismic deformation

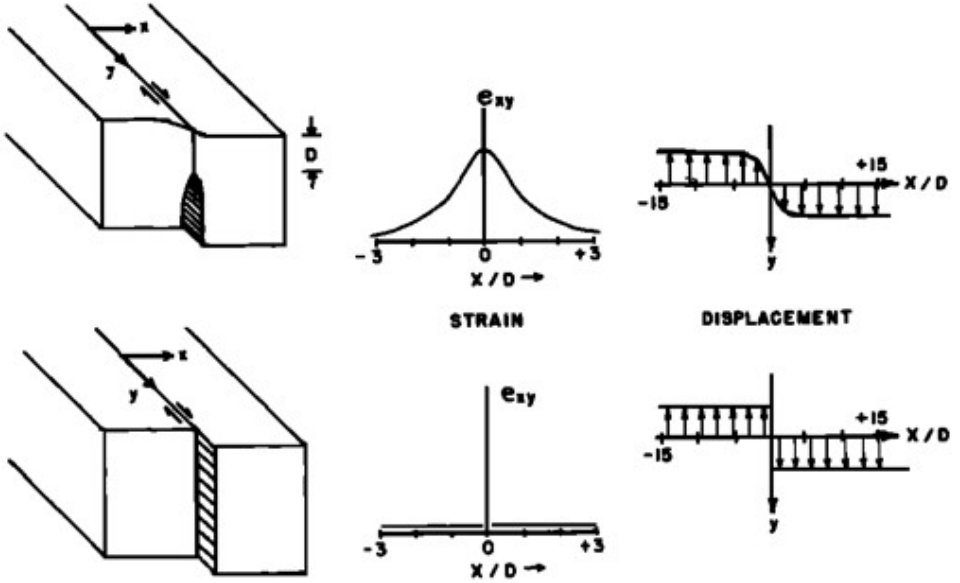

Fig. 2. Simple models for fault motion showing the distribution of shear strain and strike slip displacement on the surface. The upper sketches refer to a locked-fault model, in which slip on the fault occurs only at depths greater than D. The lower sketches refer to the rigid-block model, in which slip is approximately uniform with depth.

(Savage and Burford, 1973, Journal of Geophysical Research, 78.)

- Strike slip fault
  - Interseismic displacement pattern

$$u = \frac{\Delta u}{\pi} \tan^{-1}\left(\frac{x}{D}\right)$$

4.4. Interseismic deformation

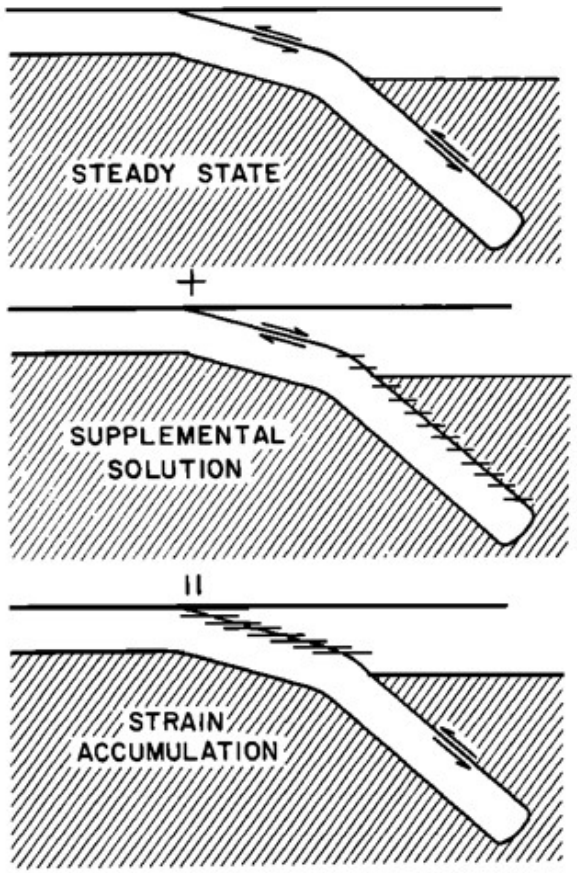

Fig. 1. Superposition model of strain accumulation at a subduction zone. The asthenosphere is indicated by shading. A locked (no slip) condition at an interface is indicated by short horizontal bars crossing the interface.

(Savage, 1983, Journal of Geophysical Research, 88.)

- Subduction zone
  - Subduction effect can be interpreted as a superposition of a steady subduction of the oceanic plate without plate interaction and a supplementary term representing plate interaction (called **slip deficit** or **backslip**)
  - Effect of the steady can be neglected in the first-order approximation

4.4. Interseismic deformation

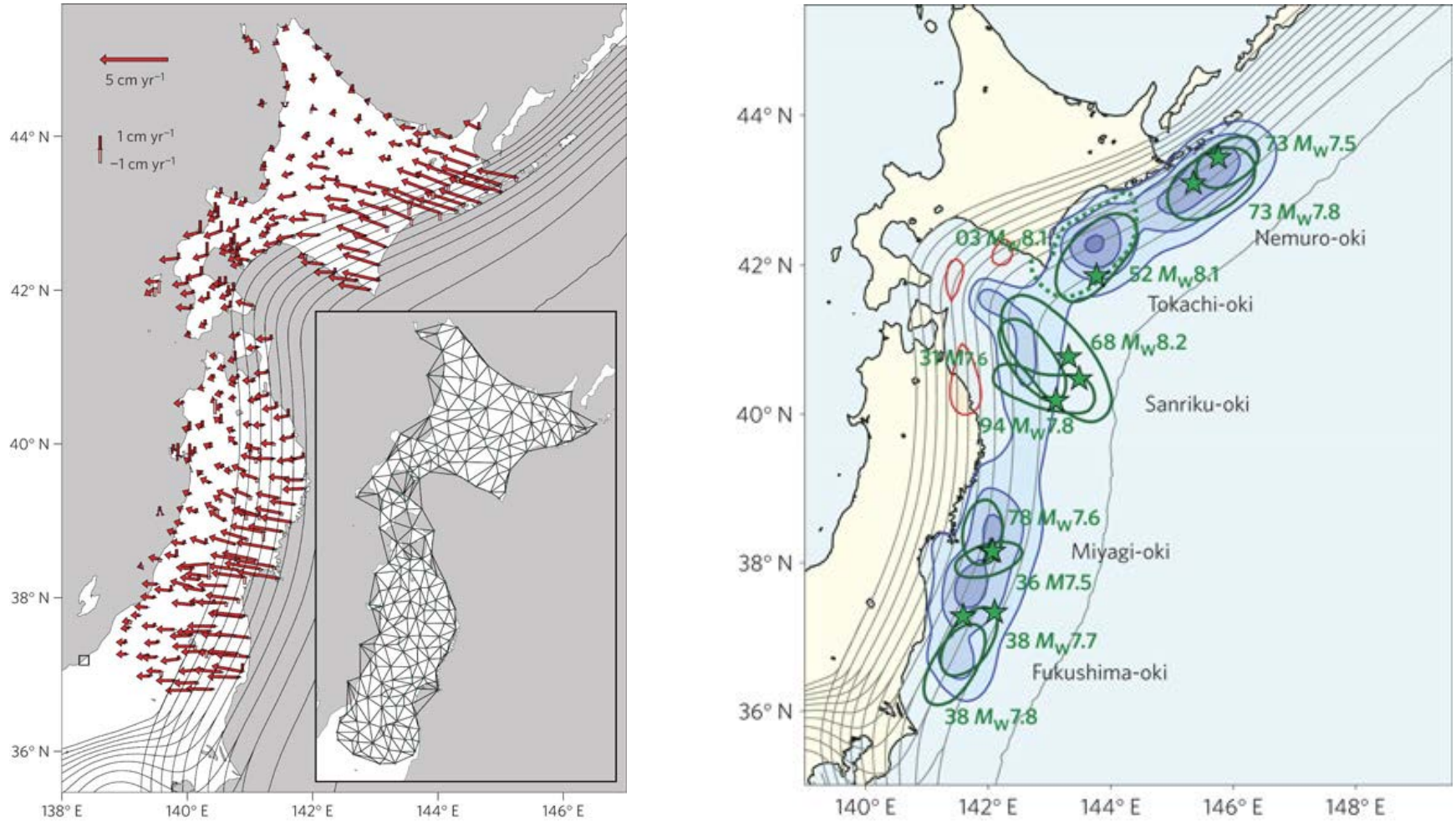

(Permission from Macmillann Publishers Ltd: Nature Geoscience, "Interplate Seismogenic Zones along the Kuril-Japan Trench Inferred from GPS Data Inversion", Hashimoto et al., 2009)

- Interplate locking zones estimated from GPS velocity data are consistent with source regions of historical earthquakes

4.5. Earthquake cycle

- Transform fault
- Repetition of interseismic strain accumulation and coseismic strain release
- Can be modeled by dislocation model

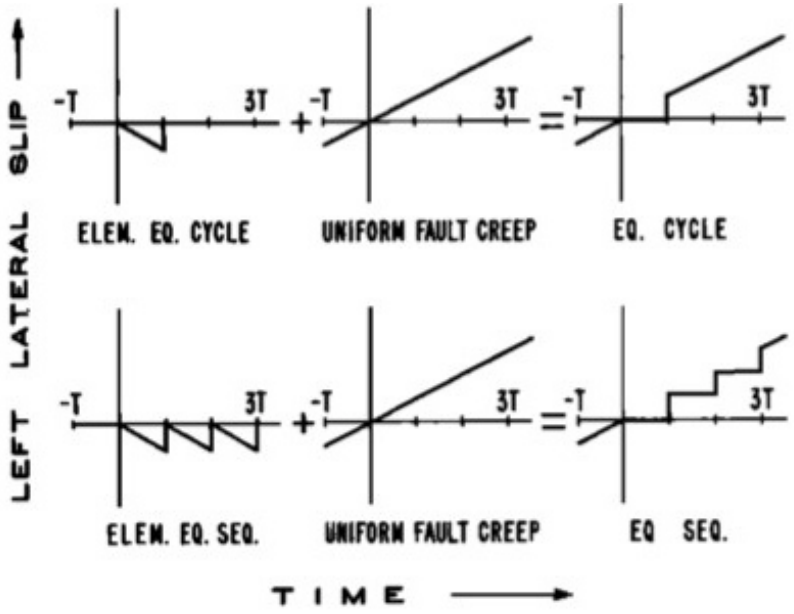

(Savage and Prescott, 1978, Journal of Geophysical Research, 83.)

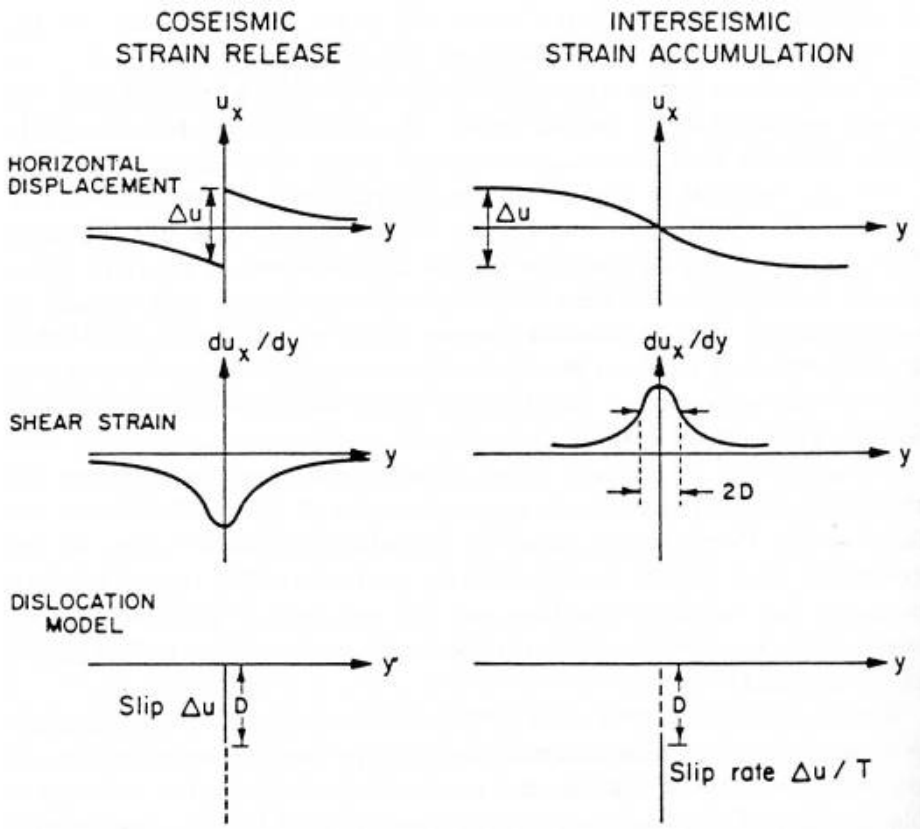

(Scholz, 2002, "The Mechanics of Earthquakes and Faulting", Cambridge University Press.)

4.5. Earthquake cycle

- Nankai trough
  - Subduction of the Philippine Sea plate
  - Recurrence of M8 class earthquakes

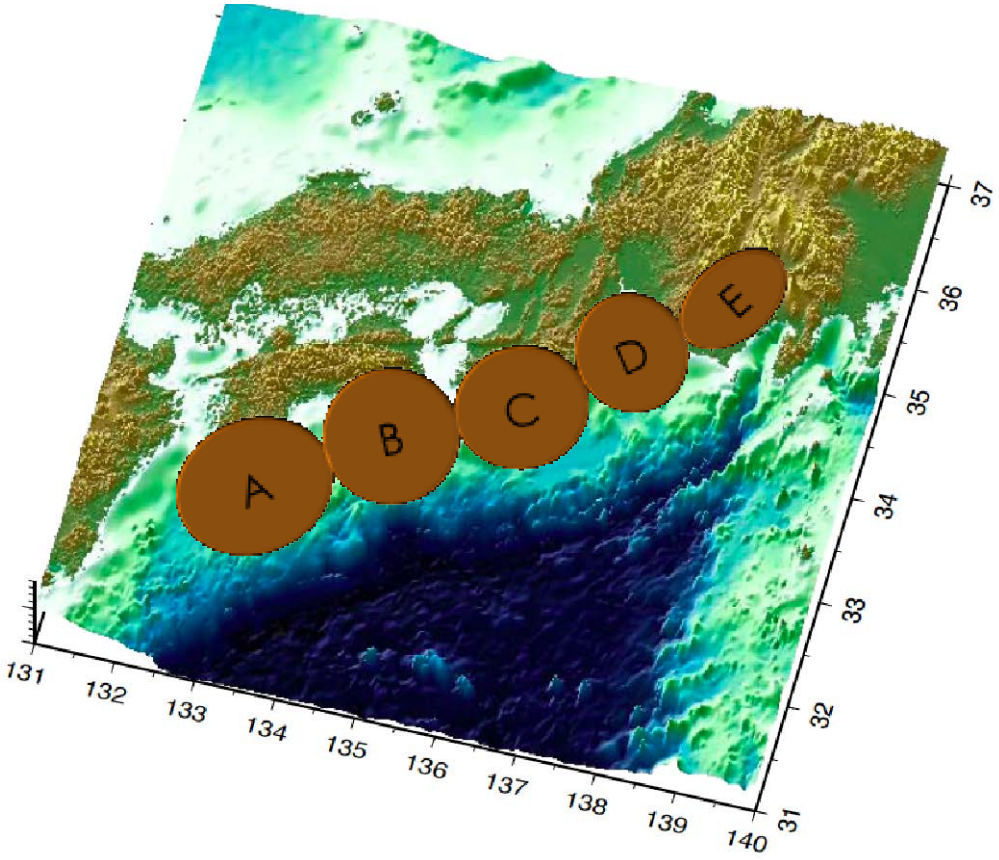

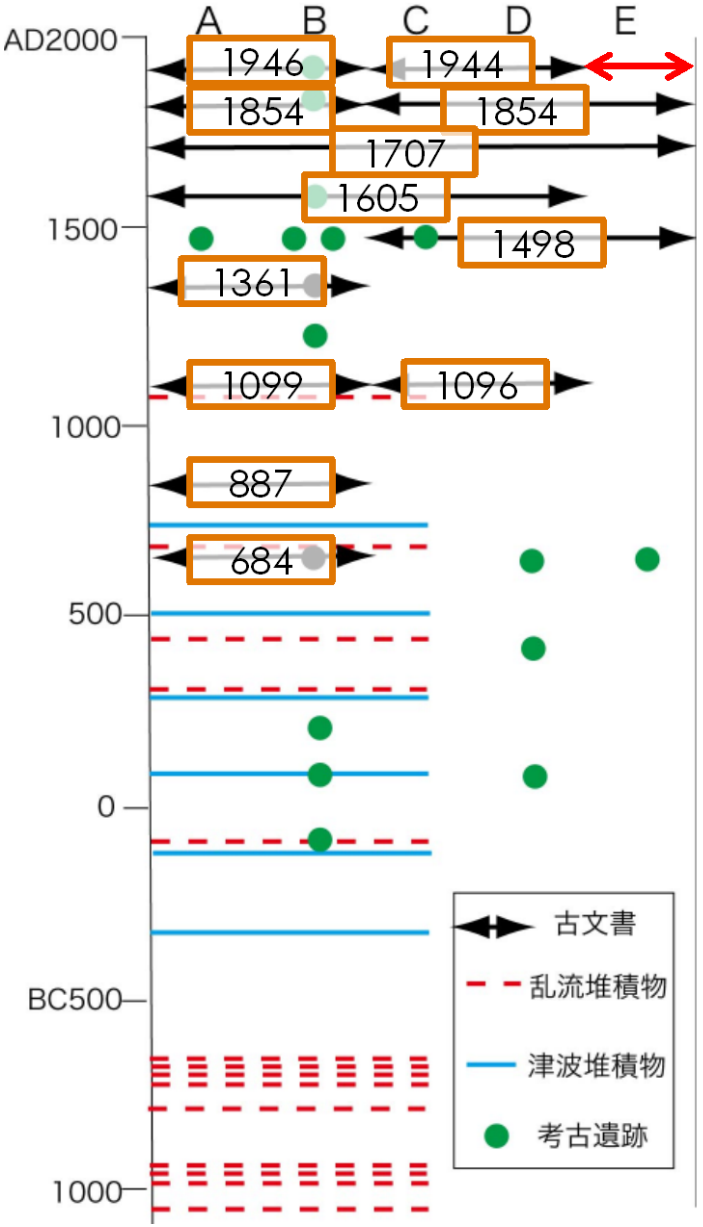

4.5. Earthquake cycle: Nankai Trough

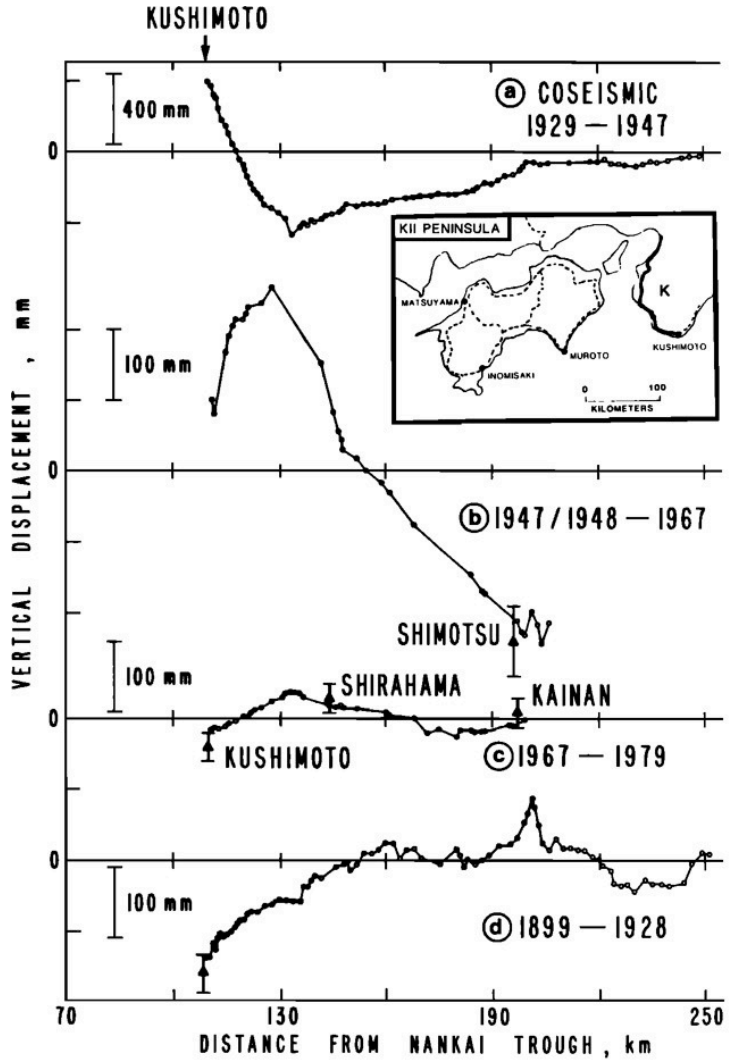

Fig. 3. Level changes on western coast of Kii Peninsula (profile K), plotted versus perpendicular distance from Nankai Trough. Note that the scale for coseismic changes differs slightly from all subsequent profiles. Triangles with error bars denote elevation changes obtained from tidal gage data.

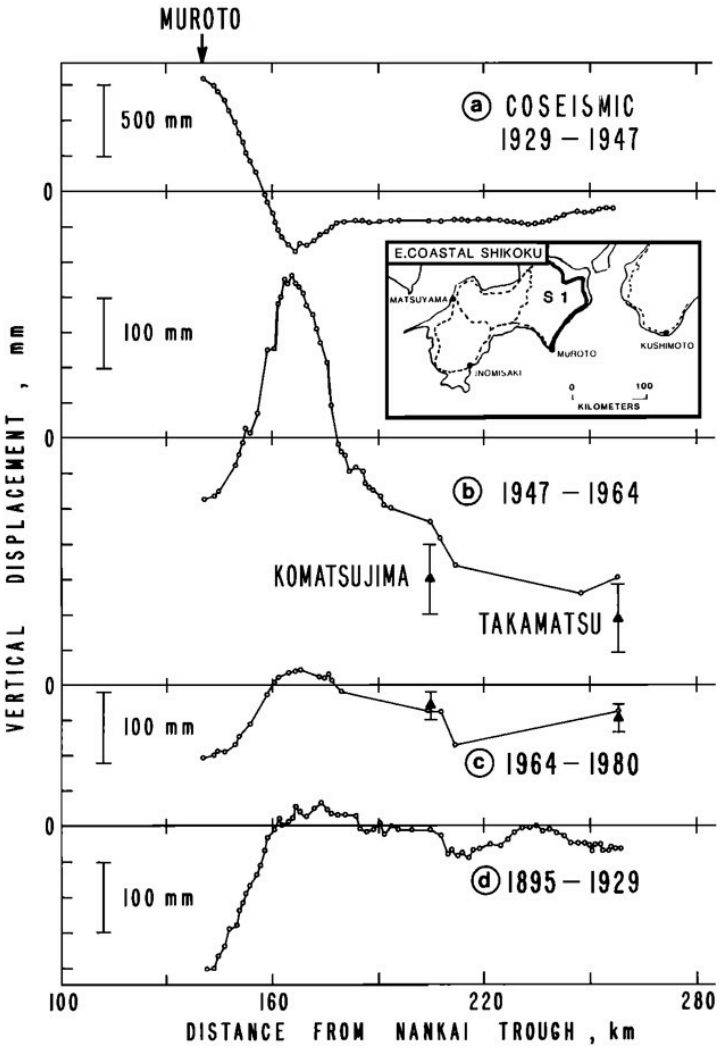

Fig. 4. Level changes on east coastal Shikoku (profile S1). Scaling and symbols for plots as in Figure 3.

(Thatcher, 1984, Journal of Geophysical Research, 89.)

4.6. Postseismic deformation

- 2003 Tokachi-oki earthquake

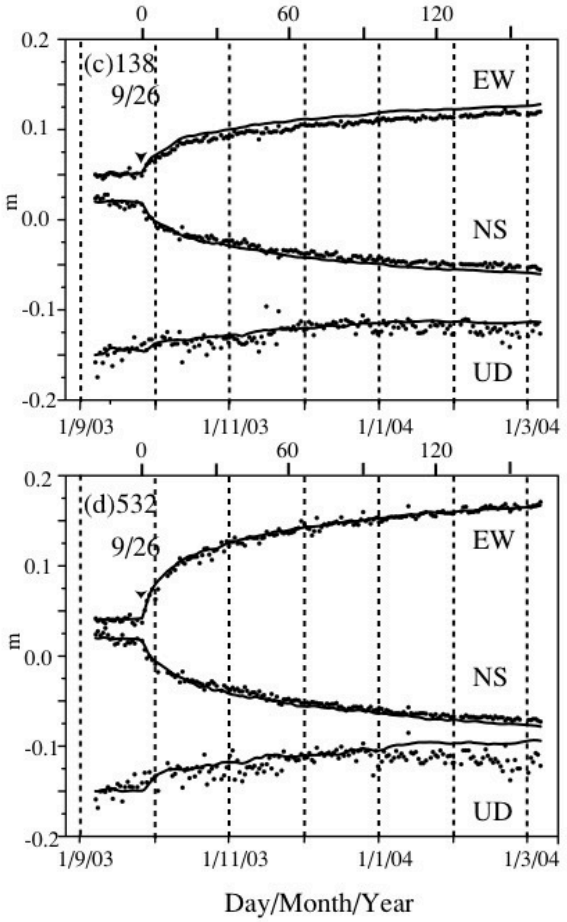

(Ozawa et al., "Coseismic and postseismic crustal deformation after the Mw 8 Tokachi-oki earthquake in Japan", Earth Planets Space, 56, 2004.)

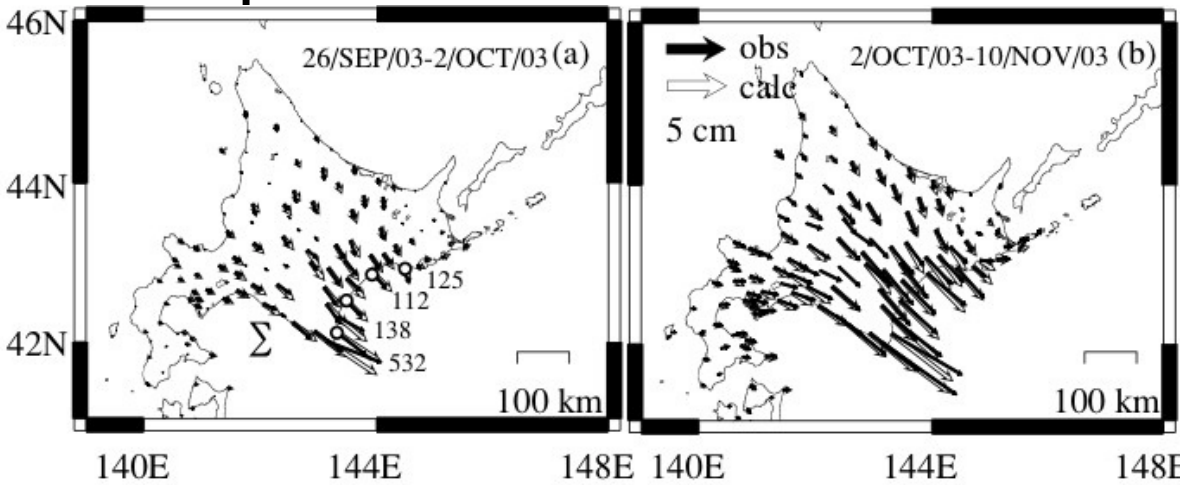

(Ozawa et al., 2004, Earth Planets Space, 56)

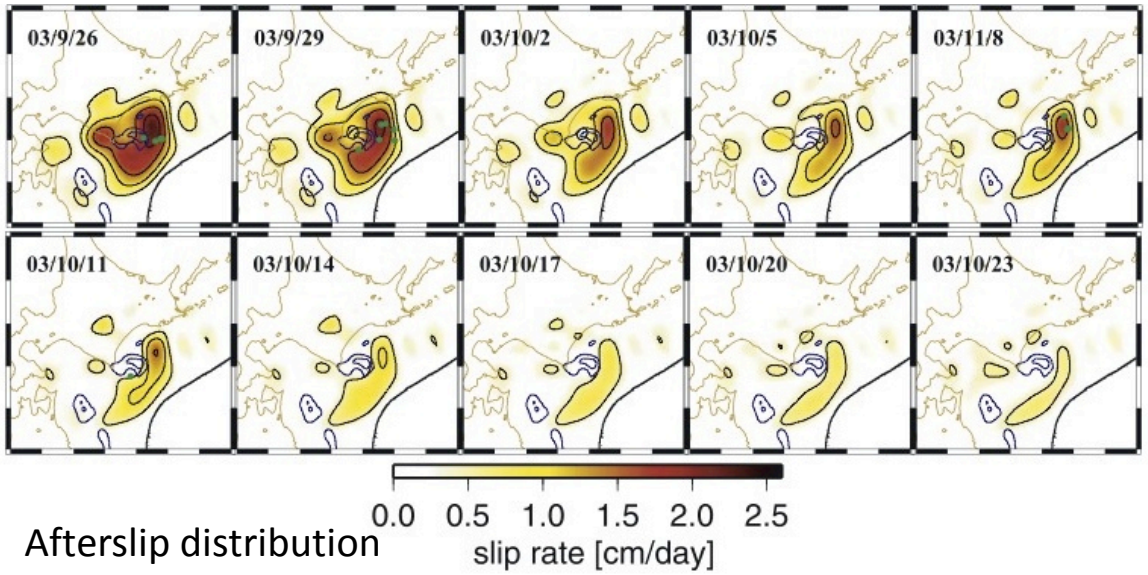

Afterslip distribution

(Miyazaki et al., 2004, Geophysical Research Letters, 31)

4.6. Postseismic deformation

- Afterslip
  - Delayed fault slip occurring on the extension of the fault plane surrounding the focal region of the main shock
  - Following a logarithmic curve

$$U = \frac{A-B}{k} \ln\left[\left(\frac{kV_{CS}^{S}}{A-B}\right)t + 1\right] + V_0 t$$

A-B: frictional parameter, k: stiffness, V^S_{CS}: coseismic slip velocity, V_0: long-term creep rate

4.6. Postseismic deformation

- Viscoelastic deformation
  - 1999 Hector Mine earthquake
  - Detected by InSAR and GPS
  - Preferable compared with other models

4.6. Postseismic deformation

- Viscoelastic relaxation
  - Viscous flow in the asthenosphere relaxes stress change caused by earthquake

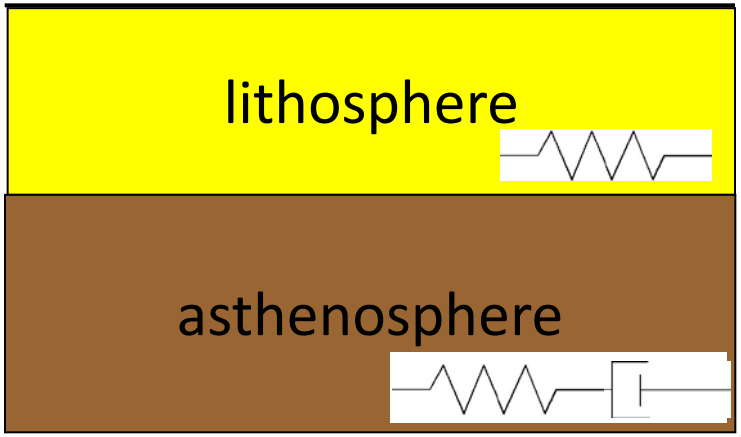

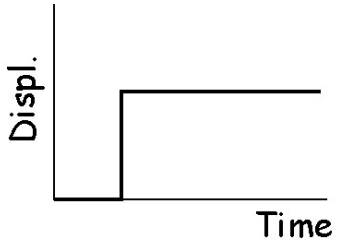

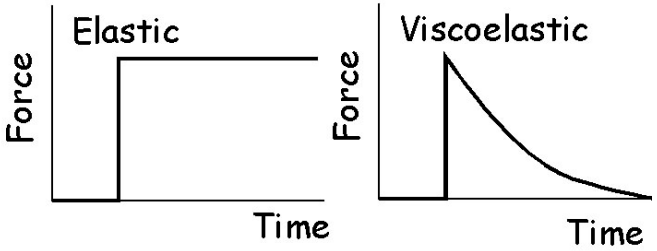

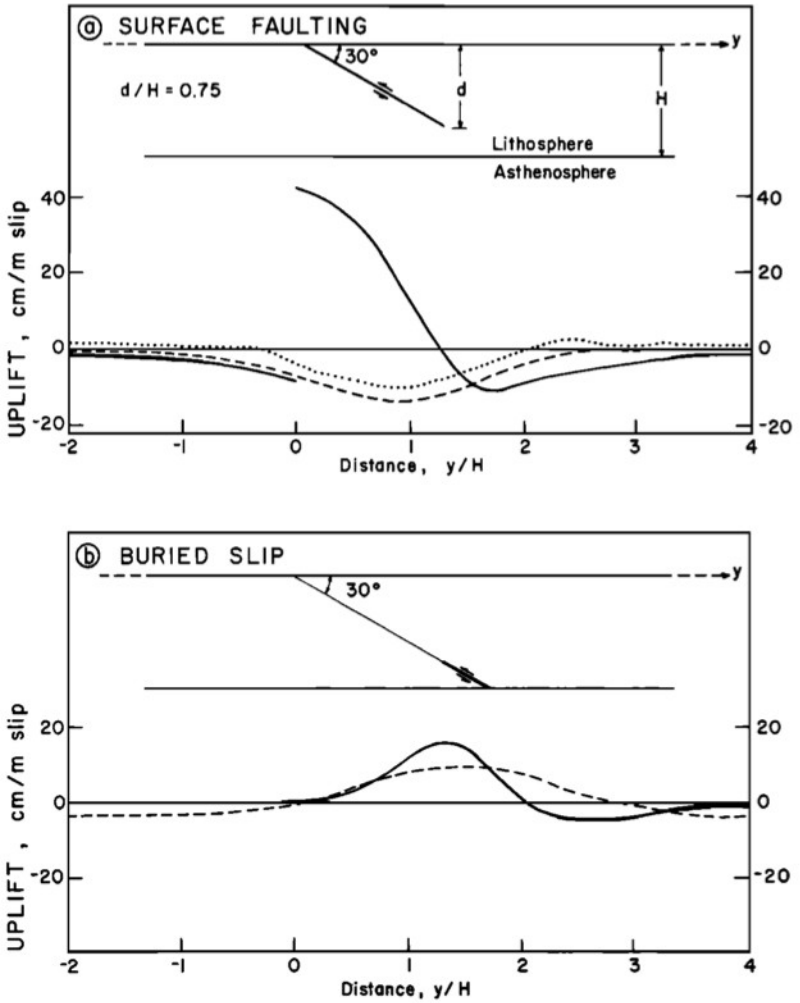

Fig. 1. (*a*) Coseismic vertical displacement ($t = 0$, solid line) and subsequent viscoelastic response ($t = 2\tau$; dotted line, compressibility of half space held constant; dashed line, λ fixed) due to slip on a fault rupturing three quarters of an elastic plate of thickness H overlying a viscoelastic (Maxwell) half space. Vertical uplift is normalized by the reverse fault slip, and distance perpendicular to the fault, y, is in multiples of the lithospheric thickness H. Fault dip is 30°. (*b*) Similar to Figure 1*a* but for buried slip extending from a depth of three quarters of the lithospheric thickness to its base.

(Thatcher and Rundle, 1979, Journal of Geophysical Research, 84.)

4.6. Postseismic deformation

- M6.5 earthquakes in Iceland
  - Rapid postseismic deformation detected by InSAR
  - Cannot be explained by afterslip or viscoelastic relaxation
  - Interpreted as a result of poroelastic rebound

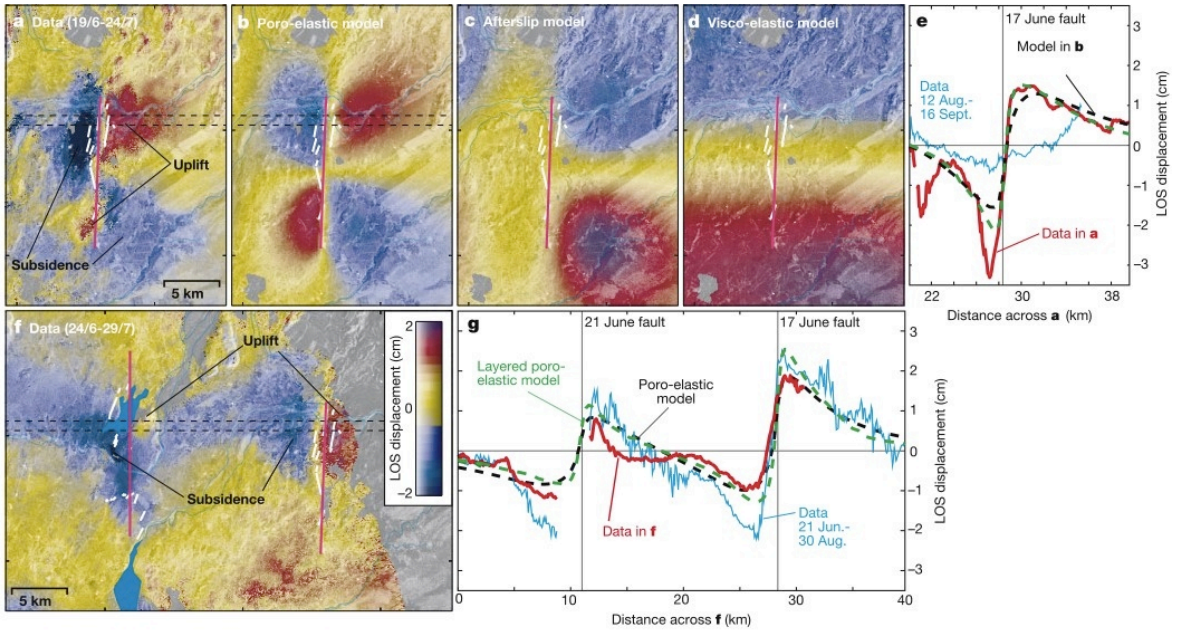

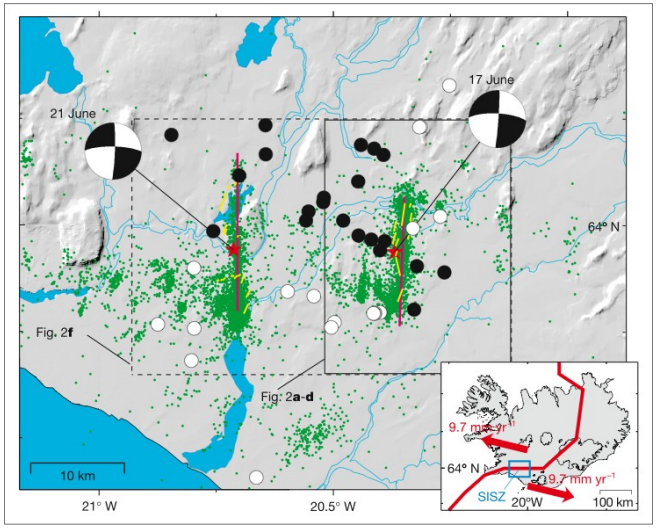

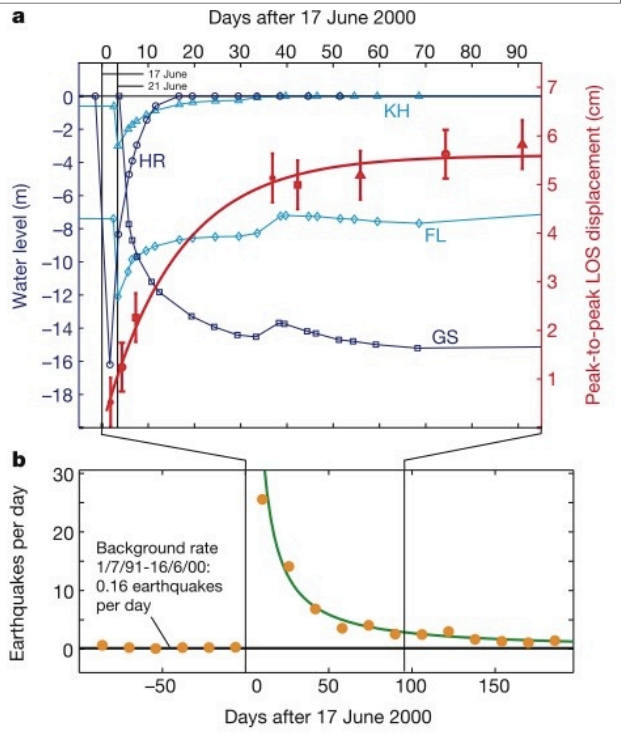

(Permission from Macmillann Publishers Ltd: Nature, "Post-Earthquake ground Movements correlated to Porepressure Transients", JÓNSSON et al., 2003.)

4.6. Postseismic deformation

- Poroelastic rebound
  - Crustal fluid flow caused by coseismic pore pressure change
  - Diffusion process reflecting permeability of the crust

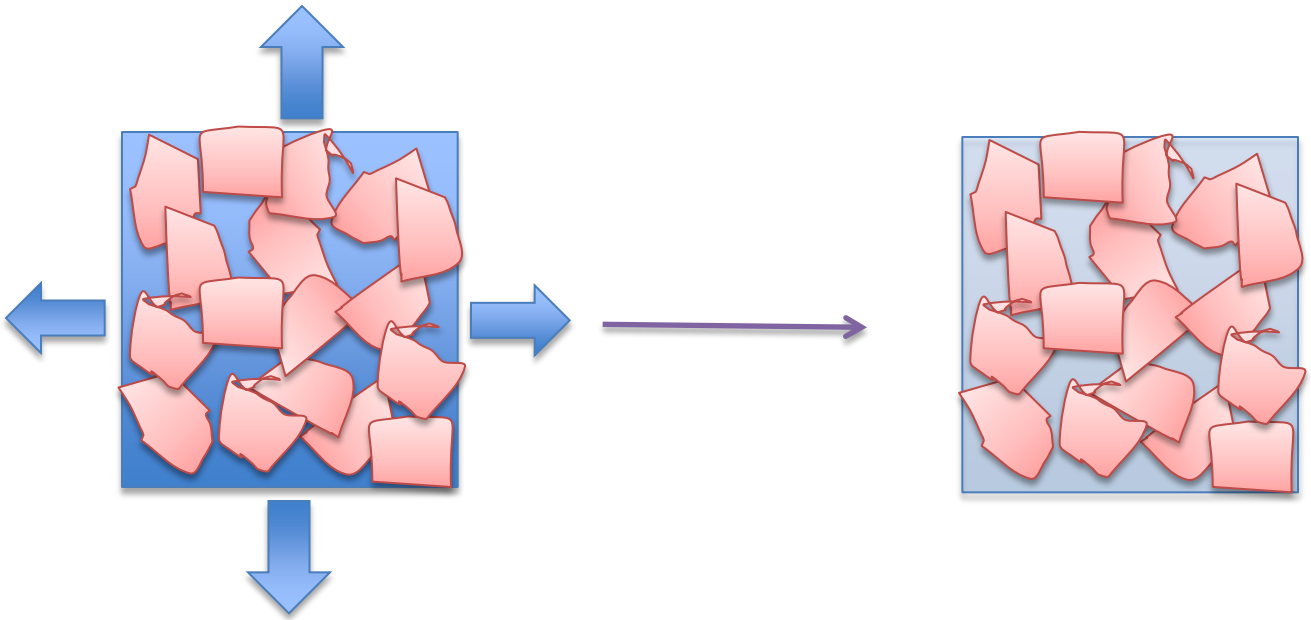

Pressure increase
➔outgoing flow

Pore pressure decrease
➔contraction

4.7. Slow slip event

- Boso slow slip in 1996
  - Slow transient motion was detected by continuous GPS
  - Max. 20mm displacement during 1 week

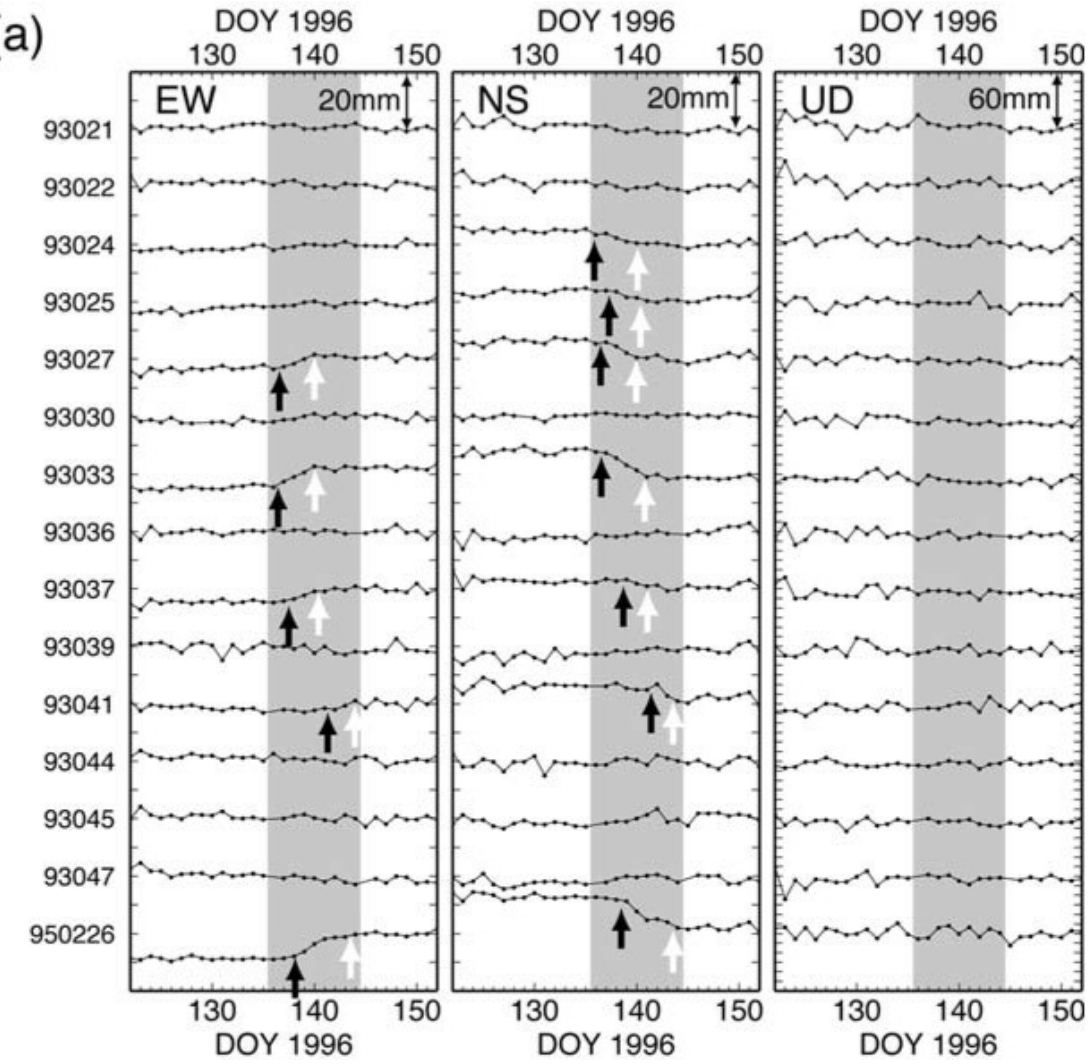

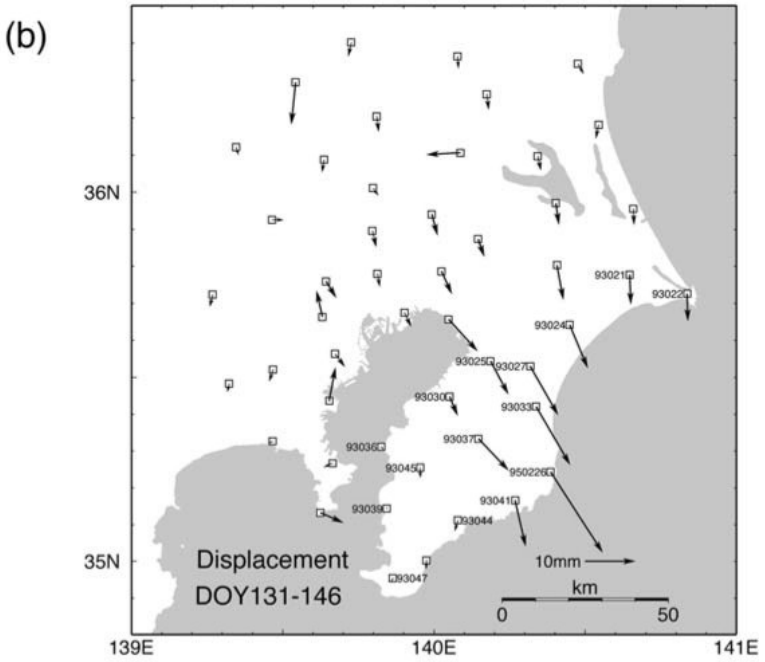

(Permission from Springer Science+Business Media: <Pure and Applied Geophysics, 161, "Interplate Coupling in the Kanto District, Central Japan, and the Boso Peninsula Silent Earthquake in May 1996", 2004, 2327-2342, Sagiya, Figures (a) and (b) on P2335>.)

4.7. Slow slip event

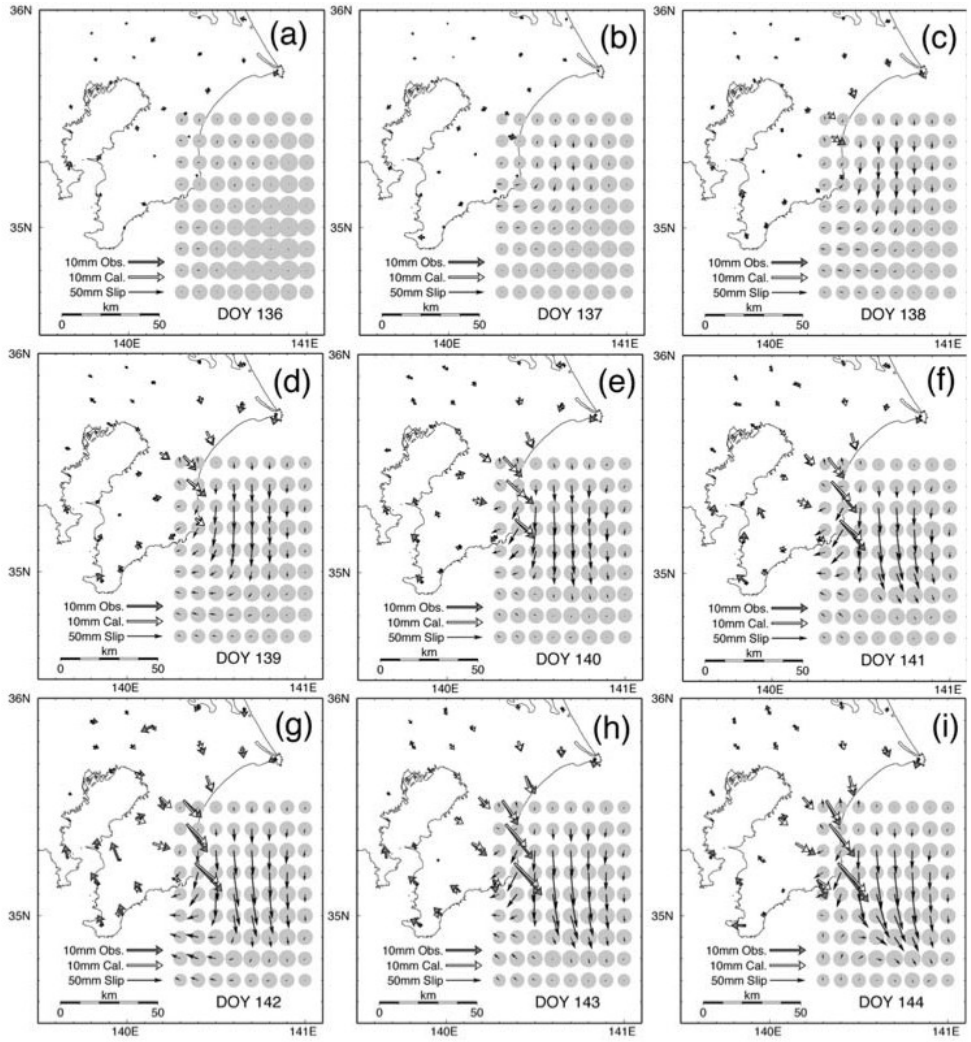

Figure 5
Daily evolution of the slip distribution on the plate boundary interface associated with the Boso silent earthquake, which is obtained by geodetic inversion analysis. Gray circles denote the estimation error (2-sigma) of the slip vectors. Gray arrows show observed displacements while the white arrows are calculated from the slip distribution.

- Boso slow slip in 1996
  - Estimated slip
  - 5cm fault slip over 50km X 50km area
  - Stress drop: 0.01MPa
  - Propagation of fault slip: 10km/day

(Permission from Springer Science+Business Media: <Pure and Applied Geophysics, 161, "Interplate Coupling in the Kanto District, Central Japan, and the Boso Peninsula Silent Earthquake in May 1996", 2004, 2327-2342, Sagiya, Figure 5 on P2337>.)

4.7. Slow slip event

- Cascadia subduction zone
  - Small offsets (~4mm) were identified in GPS time series
  - Displacement in reverse direction to the steady motion
  - Caused by slow slip on the plate boundary at depth.

4.7. Slow slip event

- Cascadia subduction zone
  - Recurrence with ~14 month interval
  - Synchronized with low frequency tremors
  - Slow slip and low frequency tremors are related events

4.7. Slow slip event

Slow slip events have been detected at circum-pacific subduction zones. Most of these events occur at the deeper extension of the megathrust earthquake source except for ones at Boso Penisula and New Zealand

a)

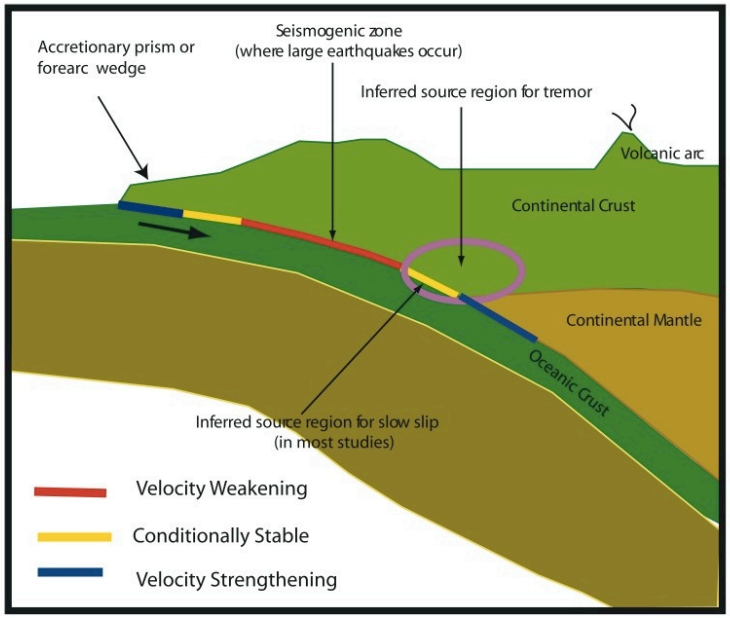

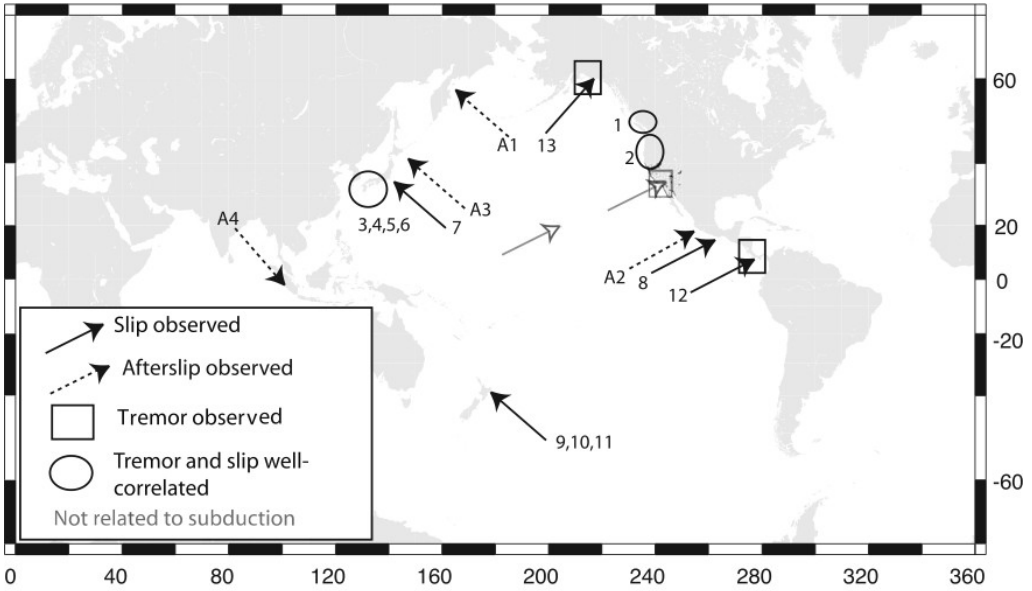

Figure 2. Map showing the location of slow slip events discussed in this review coded to represent interseismic slip (solid arrows), afterslip (dashed arrows), and slip not related to subduction (shaded arrows). The numbers correspond to those listed in Table 1. Circles and boxes represent regions where seismic tremor has been observed and is or is not well correlated with slow slip, respectively.

(Schwartz and Rokosky, 2007, Reviews of Geophysics, vol.45.)

4.8. Static stress change

- Earthquake deformation is accompanied with stress redistribution of the medium
- If we consider a fault, both the shear stress and the normal stress are affected by a large earthquake.
- Coulomb Failure Function (ΔCFF)
  - Evaluate stress change effect on a fault rupture
  - Combined effect of shear stress change ($\Delta\sigma_n$)and normal stress change ($\Delta\tau_s$)

$$CFF = \tau_s - \mu(\sigma_n - p)$$

$$\cong \tau_s - \mu'\sigma_n$$

$$\Delta CFF = \Delta\tau_s - \mu'\Delta\sigma_n$$

μ: friction coefficient

μ': effective friction coefficient

p: pore pressure

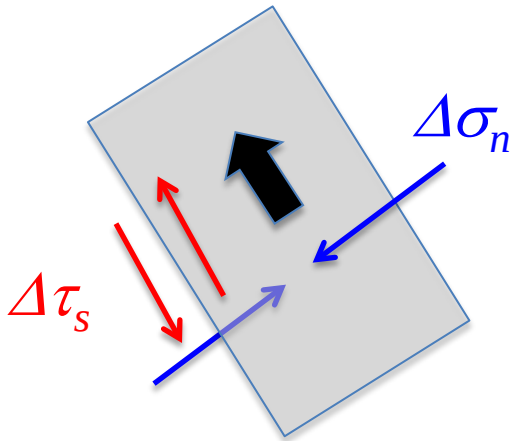

4.8. Static stress change

- Shear stress change and normal stress change have different effect on the receiver fault
- Two way of evaluating stress change
  - Evaluate ΔCFF on a prescribed fault mechanism
  - Evaluate ΔCFF on a optimally oriented fault at each point

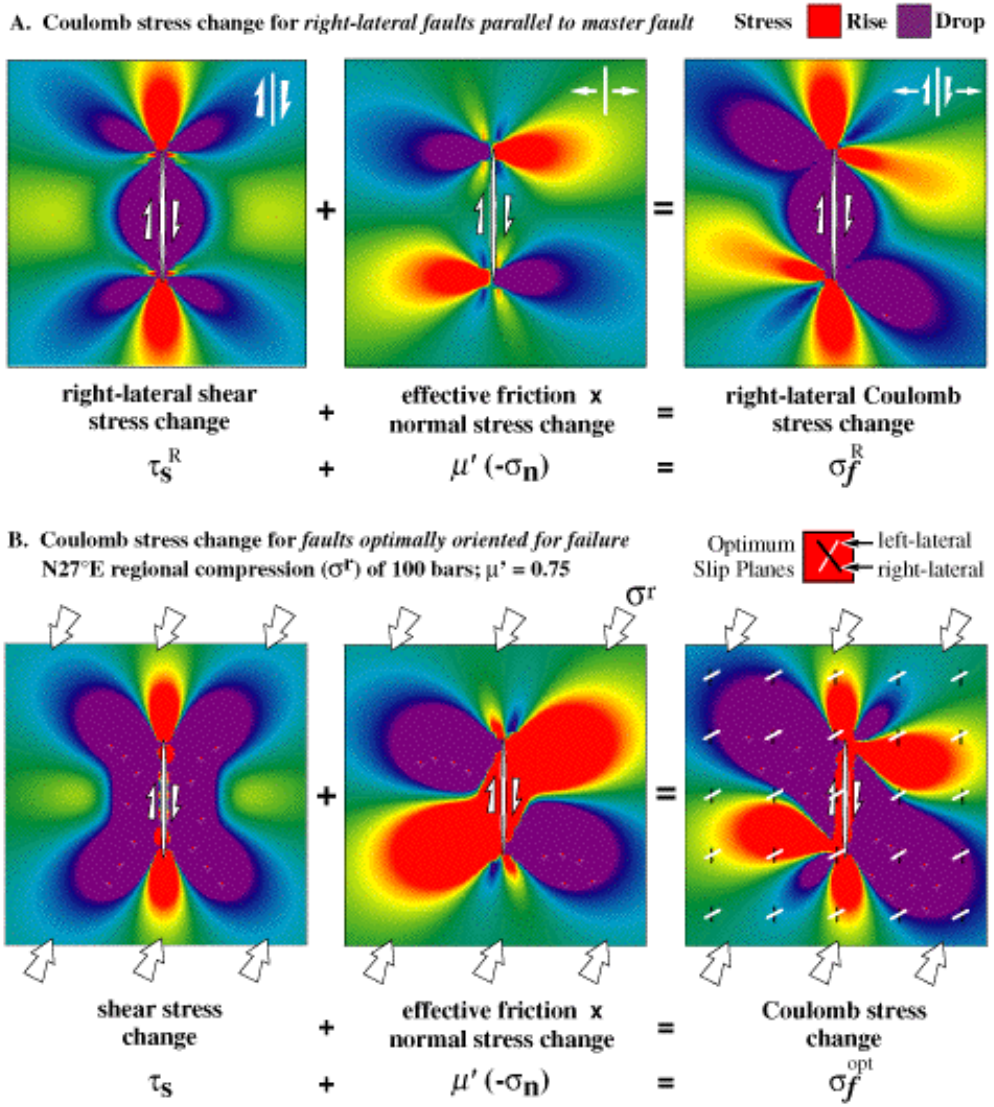

(King et al., Bulletin of the Seismological Society of America, vol.84, 1994)

4.8. Static stress change

- 1992 Landers earthquake
  - The largest after shock (M6.5 Big Bear earthquake) occurred in the positive ΔCFF region
  - Small aftershocks are concentrated in the positive ΔCFF region
  - ΔCFF is a good measure to evaluate earthquake triggering effect

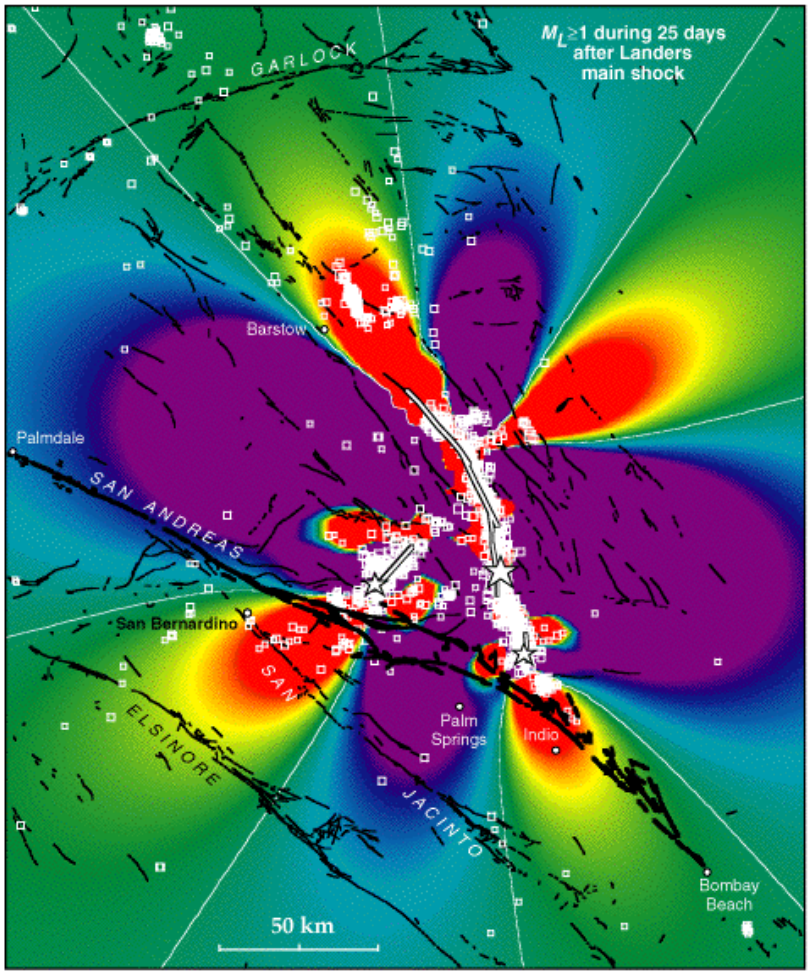

(King et al., Bulletin of the Seismological Society of America, vol.84, 1994)

4.8. Static stress change

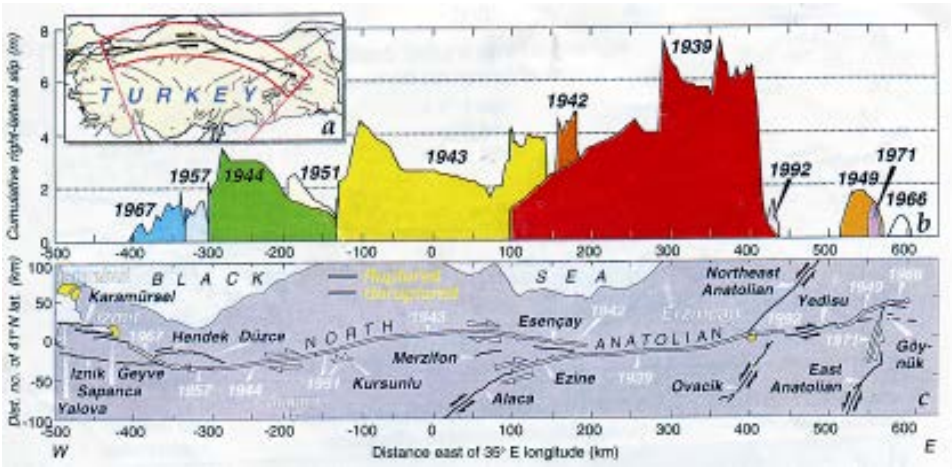

- North Anatolian Fault in Turkey
  - Sequence of large earthquakes since 1939 was interpreted in terms of triggering.
  - 1999 Izmit earthquake occurred where seismic risk was considerably high (30 year probability of 12%) due to stress change due to the sequence.

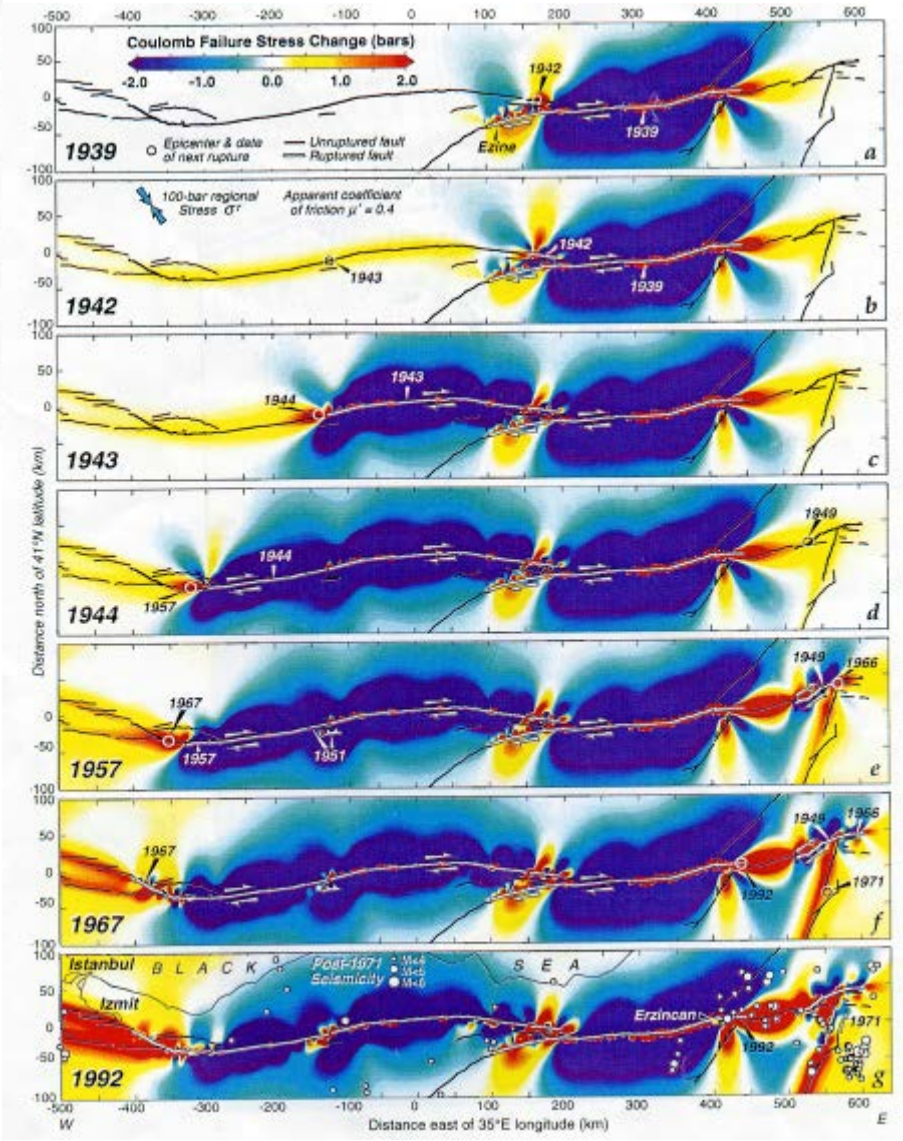

(Stein et al., Geophysical Journal International, vol.128, 1997.)

4.8. Static stress change

1999 Duzce earthquake occurred where 1999 Izmit earthquake raised seismic potential.

Another stressed region exists in the eastern Marmara Sea.

5. Volcanic deformation

- Point inflation source (Mogi model)
  - Deep inflation source

$$dr = \frac{\Delta V}{2\pi}\frac{\lambda+2\mu}{\lambda+\mu}\frac{r}{\left(r^2+D^2\right)^{3/2}} \qquad dh = \frac{\Delta V}{2\pi}\frac{\lambda+2\mu}{\lambda+\mu}\frac{D}{\left(r^2+D^2\right)^{3/2}}$$

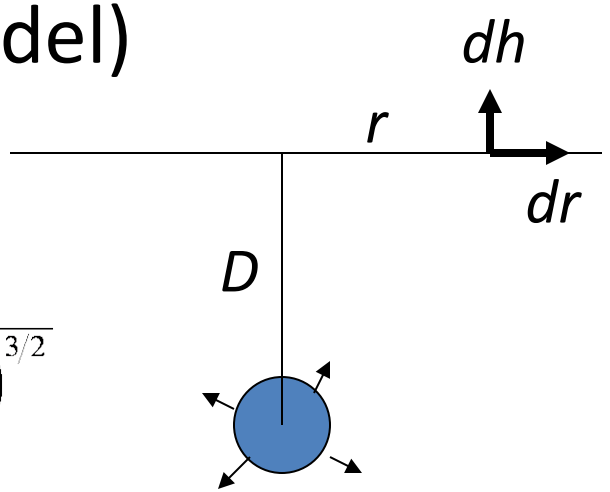

- Tensile fault
  - Shallow inflation source reflecting regional stress field
  - Formula was already presented in earthquake deformation